


IMPACT OF GROWTH PHASE, PIGMENT ADAPTATION, AND CLIMATE CHANGE CONDITIONS ON THE CELLULAR PIGMENT AND CARBON CONTENT OF FIFTY-ONE PHYTOPLANKTON ISOLATES¹

Aimee R. Neeley ²

NASA Goddard Space Flight Center/Science Systems and Applications Inc., Greenbelt, Maryland 20771, USA

Michael W. Lomas

Bigelow Laboratory for Ocean Sciences, Bigelow Institute of Ocean Sciences, East Boothbay, Maine 04544, USA

Antonio Mannino

NASA Goddard Space Flight Center, Greenbelt, Maryland 20771, USA

Crystal Thomas, and Ryan Vandermeulen

NASA Goddard Space Flight Center/Science Systems and Applications Inc., Greenbelt, Maryland 20771, USA

Owing to their importance in aquatic ecosystems, the demand for models that estimate phytoplankton biomass and community composition in the global ocean has increased over the last decade. Moreover, the impacts of climate change, including elevated carbon dioxide (CO₂), increased stratification, and warmer sea surface temperatures, will likely shape phytoplankton community composition in the global ocean. Chemotaxonomic methods are useful for modeling phytoplankton community composition from marker pigments normalized to chlorophyll *a* (Chl *a*). However, photosynthetic pigments, particularly Chl *a*, are sensitive to nutrient and light conditions. Cellular carbon is less sensitive, so using carbon biomass instead may provide an alternative approach. To this end, cellular pigment and carbon concentrations were measured in 51 strains of globally relevant, cultured phytoplankton. Pigment-to-Chl *a* and pigment-to-carbon ratios were computed for each strain. For 25 strains, measurements were taken during two growth phases. While some differences between growth phases were observed, they did not exceed within-class differences. Multiple strains of *Amphidinium carterae*, *Ditylum brightwellii* and *Heterosigma akashiwo* were measured to determine whether time in culture influenced pigment and carbon composition. No appreciable trends in cellular pigment or carbon content were observed. Lastly, the potential impact of climate change conditions on the pigment ratios was assessed using a multistressor experiment that included increased mean light, temperature, and elevated pCO₂ on three species: *Thalassiosira oceanica*, *Ostreococcus lucimarinus*, and *Synechococcus*. The largest

differences were observed in the pigment-to-carbon ratios, while the marker pigments largely covaried with Chl *a*. The implications of these observations to chemotaxonomic applications are discussed.

Key index words: carbon; chemotaxonomy; climate change; cyanobacteria; diatoms; dinoflagellates; growth phase; high-performance liquid chromatography; phytoplankton; pigments

Abbreviations: CC, climate change; ExpP, Exponential phase; fmol, femtomoles; mM, millimolar; n.d., not detected; PCC, Phytoplankton community composition; Pig, Pigment; pmol, picomoles; StatP, Stationary phase; Td, doubling time

Aquatic phytoplankton are a vital source of food for many aquatic organisms and are responsible for roughly one-half of global primary productivity (Field et al. 1998, Falkowski and Raven 2007), influence biogeochemical cycles (Falkowski 1994, Litchman et al. 2015), and mediate rates of carbon sequestration and export (Barton et al. 2020). The continued rise in atmospheric CO₂ concentrations and warming ocean temperatures will have a significant impact on ocean ecosystems and phytoplankton community composition (PCC), in particular, by means of ocean acidification and enhanced stratification. Increased stratification leads to exposure of phytoplankton to increased light levels, warmer waters, and decreased nutrient availability owing to less mixing with the deep ocean where nutrients are regenerated. The combination of ocean acidification, warming and stratification will likely lead to physiological changes in phytoplankton as well as competitive outcomes PCC that will impact the oceanic food web, carbon sequestration, and carbon export (Feng et al. 2009, Low-

¹Received 3 December 2021. Accepted 22 June 2022.

²Author for correspondence: e-mail aimee.neeley@nasa.gov
Editorial Responsibility: A.M. Wood (Associate Editor)

Decarie et al. 2011, Xu et al. 2014, Rivero-Calle et al. 2015).

Satellite remote sensing methods have evolved over the last 20+ years, from estimating chlorophyll *a* (Chl *a*) as a proxy for phytoplankton biomass (O'Reilly et al. 1998, O'Reilly and Werdell 2019), to the development of more advanced methods that estimate PCC at both taxonomic (Bracher et al. 2009, Sadeghi et al. 2012) and size class level (Ciotti and Bricaud 2006, Uitz et al. 2006). Satellite-derived Chl *a* has become an invaluable tool for tracking global trends in phytoplankton biomass. Recent studies have indicated that a large-scale decline in phytoplankton biomass has occurred in the subtropical gyres (Signorini et al. 2015) while phytoplankton biomass has increased in the Southern Ocean (Del Castillo et al. 2019). Estimates of Chl *a* as a proxy for phytoplankton biomass are not always reliable as this photosynthetic pigment is sensitive to various environmental factors, such as light and nutrient regimes, as well as biological factors, including cell size and the "package effect" (Duyens 1956, Lohrenz et al. 2003). Phytoplankton-specific carbon is a more reliable indicator of phytoplankton biomass than Chl *a* because it is not as sensitive to fluctuations in phytoplankton photo-physiology, but, historically, has been more difficult to obtain. Recent technological and methodological advances, such as the use of flow cytometric sorting and direct (Graff et al. 2012) as well as indirect (Casey et al. 2013) estimates of cellular carbon, will likely increase the frequency of the phytoplankton carbon measurements.

Current efforts are underway to develop remote sensing algorithms and ecosystem models that estimate both Chl *a* and carbon-based phytoplankton biomass, as well as PCC and diversity, by utilizing hyperspectral ocean color data that will be available from future satellite missions, including NASA's upcoming Plankton, Aerosol, Cloud, ocean Ecosystem (PACE) mission (Werdell et al. 2019). Operational ocean color algorithms that elucidate PCC and diversity will be important tools in the effort to quantify the ecological impacts from global environmental change and variability. Ocean observations of PCC are also necessary for algorithm development and validation. High-performance liquid chromatography (HPLC) measurements of phytoplankton pigments provide a link to the optical signature of phytoplankton that is detectable from space. Marker or diagnostic pigments are used routinely to characterize PCC, a method known as chemotaxonomy. The use of HPLC in pigment determinations has played a key role in the development and validation of PCC and size class models and algorithms (Uitz et al. 2006, Hirata et al. 2011, Chase et al. 2017). Mathematical tools, such as Inverse Simultaneous Equations (Letelier et al. 1993) and the CHEMical TAXonomy or CHEM-TAX program (Mackey et al. 1996), have been

developed to interpret marker pigments normalized to Chl *a* (Pig/Chl *a*) to quantify the abundance of taxonomic groups relative to total Chl *a* biomass. Using pigment ratios and/or pigment-to-biomass ratios could provide a powerful tool for developing and ground truthing algorithms that derive community composition.

The Phytoplankton Library of Optical Properties and Spectra project was developed to build a comprehensive library of phytoplankton pigments, pigment ratios, and other bio-optical properties (including measurements of absorption and scattering) that will support advanced approaches currently under development to derive PCC in the global ocean from hyperspectral ocean color data. The 51 strains chosen for the project are representatives of each major phytoplankton taxonomic group in the global ocean and cover both coastal and open ocean ecosystems. Additionally, the strains were chosen in anticipation that they would be challenging for modeling approaches that use pigments or pigment ratios to resolve in the context of the observed remote sensing reflectance (R_{rs}) because they express similar pigment profiles or are comparatively similar in cell size. In this paper we present an extensive library of Pig/Chl *a*, pigment-to-carbon (Pig/C), and C/Chl *a* ratios developed from this project. The advantage of normalizing to carbon instead of Chl *a* is that cellular carbon, unlike Chl *a*, is not susceptible to short-term light variability (Schlüter et al. 2000), thereby providing a more stable approach to examining pigment ratios across phytoplankton taxa. The Pig/C and C/Chl *a* ratios measured during this project will be particularly useful for advanced algorithms and models that will derive PCC from particulate carbon pools. Pigment ratios between two growth phases, mid-exponential and stationary, will be presented for a subset of the strains to assess species-specific physiological responses under both nutrient limiting (stationary) and nonlimiting (mid-exponential) growth conditions. Secondly, a pigment adaptation study was implemented, where the pigment and carbon profiles for multiple strains of three different species were measured to determine if length of time in culture influenced pigment composition and the pigment ratios. Previous studies, as described in Wood and Leatham (1992) and Lakeman et al. (2009) and references therein, show that phytoplankton grown under controlled laboratory conditions as opposed to the natural environment exhibit some changes in physiology. Adaptations with respect to pigments has not been similarly explored and will be addressed in this study. Any additional uncertainties in the pigment ratios associated with the different growth conditions or pigment adaptation will be discussed with relation to chemotaxonomic analyses. Additionally, intraspecific and interspecific group comparisons of shared marker pigment ratios are briefly discussed for chemotaxonomic applications. Lastly, the results

of a multistressor experiment that examined the impact of elevated light, temperature, and pCO₂ on Pig/Chl *a*, Pig/C ratios, and C/Chl *a* ratios are reported.

MATERIALS AND METHODS

Culturing methods. The strains chosen for this study were cultivated at the National Center for Marine Algae and Microbiota (NCMA) at the Bigelow Laboratory for Ocean Sciences and are from regions where they are known to occur currently (e.g., diatoms from the North Atlantic, cyanobacteria from the oligotrophic gyres) to serve as a positive control for the new algorithms to be developed (Table 1). Cultures were grown axenically on a 14:10 h L:D cycle, and at 80 $\mu\text{mol photons} \cdot \text{m}^{-2} \cdot \text{s}^{-1}$ for the warmer growth temperatures ($>14^\circ\text{C}$) and $\sim 50 \mu\text{mol photons} \cdot \text{m}^{-2} \cdot \text{s}^{-1}$ at the cooler growth temperatures ($<10^\circ\text{C}$). Most strains were grown using L1 medium (Guillard and Hargraves 1993), which has a more complex array of trace metals than found in f/2 medium. *Prochlorococcus marinus* was grown in Pro99 medium (Moore et al. 2007), which contains sodium phosphate, ammonium chloride, and trace elements. Each culture was maintained in a semi-continuous state in 0.5 L Erlenmeyer flasks to align cellular physiological state within the population as much as practical without the use of chemostats. Cell counts were made through one growth or dilution cycle for each culture to determine at what frequency a given culture would need to be diluted. When possible, samples were counted on a hemocytometer (Guillard 1973). Strains smaller than $\sim 3 \mu\text{m}$ were counted by flow cytometry (Lomas et al. 2013). At least 200 cells were counted to keep the error to $<10\%$. In subsequent growth or dilution cycles and *in vivo* Chl *a* fluorescence was measured to track biomass and determine the timing of dilution. Each stock culture was acclimated for approximately 10 divisions (~ 3 divisions dilution cycle⁻¹) to minimize self-shading through exponential phase. Images of cells were processed with AxioVision Release 4.9.1. Cells were measured using the software function calibrated to a stage micrometer for each objective. To calculate cell biovolume, the volume of a cylinder was used for the diatoms, where cell height in girdle view was assumed to be equal to the diameter, while the diameter was assumed to be equal to the height when in valve view. For all other cells, the volume was assumed to be that of an ovoid if the major and minor axes were different or a sphere when the axes were the same.

For most of the strains, measurements were made at two growth stages: mid-exponential (ExpP) and stationary (StatP) growth phase. For a select number of strains, measurements were made during only one growth phase to increase the number of strains for the optical fingerprint library. Growth curves for most of the cultures (data not shown) exhibited a typical sigmoid shape where the two growth phases could be clearly defined. Cell biovolume, growth rate (μ , d⁻¹), and doubling time (Td, d) for each strain can be found in Table 1.

Prior to performing the bio-optical and biogeochemical measurements, the concentrated stock cultures were quantitatively diluted to natural phytoplankton bloom cell densities in two 25 L carboys using filtered ($<0.2 \mu\text{m}$) saline Damariscotta River water (32–33 salinity) and class A volumetric flasks and graduated cylinders. The purpose of diluting the cultures in large volumes was to (i) create enough volume for the various optical measurements and sample collection and (ii) to avoid saturating the signal to the optical sensors. Each carboy was stirred thoroughly and subsampled for chemical characterization, including particulate organic carbon and

pigments, cell enumeration, and discrete particle absorption measurements so that the biogeochemical measurements, including pigments, could be directly related to the optical measurements. Replicate filters were collected from each carboy. The reported uncertainties for pigment and carbon measurements includes both the uncertainty between the carboys and the replicate sample filters from each carbon.

POC sampling and measurement. Phytoplankton particulate organic carbon (C), nitrogen (N), and phosphorus (P) measurements are important for context and understanding the relationships between pigments and phytoplankton carbon. Samples for C/N/P were filtered on pre-combusted (450°C, 4 h) Sterlitech GF-75 filters and frozen until analysis. C/N samples were acid fumed overnight and analyzed on a COST-ECH 4010 elemental analyzer using acetanilide as a standard (Lomas et al. 2013). Dissolved organic C, N, and P are known to adsorb to filters resulting in overestimation of particulate C, N, and P measurements. This uncertainty was quantified, and measurements corrected, by passing an equivalent volume of cell-free spent media through a pre-combusted filter. Phytoplankton biomass comprised $>99\%$ of the C, N, and P measured in each culture as bacteria are either not present (axenic cultures) or found in very low abundances.

HPLC pigments sampling and measurement. Samples for pigment analysis were filtered onto glass fiber filters, placed in aluminum foil pouches, and immediately stored in liquid nitrogen. For long-term storage, samples were kept at -80°C . Phytoplankton pigments (Table 2) were determined using high-performance liquid chromatography (HPLC) following the procedures of Van Heukelem and Thomas (2001) and further described in Hooker et al. (2005). Briefly, 2.5 mL of 100% acetone (includes the internal standard Vitamin E acetate) and 0.15 mL of water were added to filters for a final acetone concentration of 90%. Samples were disrupted using an ultrasonic probe. Extraction soaking time was 4 h at -25°C . Samples were clarified through a $0.45 \mu\text{m}$ pore size syringe filter before analysis. The pigments were analyzed on an Agilent RR1200 HPLC with a $4.6 \times 150 \text{ mm}$ Eclipse XDB C8 column, refrigerated autosampler compartment, thermostatted column compartment, quaternary pump with in-line vacuum degasser, and photo-diode array detector with deuterium and tungsten lamps, which collects in-line visible absorbance spectra for each pigment. The mobile phase consisted of a linear gradient from 5 to 95% solvent B over 27 min, for which solvent A is 70 parts methanol/30 parts 28 mM tetrabutylammonium acetate (pH 6.5) and solvent B is methanol. The column temperature was 60°C , and Vitamin E acetate was used as the internal standard for determining extraction volumes.

A total of 24 pigments were identified in this study. The pigments detected by HPLC analysis, and their abbreviations are listed in order of retention time in Table 2. The abbreviations adhere to the labeling scheme put forth in (Jeffrey 1997, Roy et al. 2011) with the exception of chlorophylls *c1* and *c2* (Chl *c1c2*) that is a designation specific to the HPLC analysis laboratory at NASA Goddard Space Flight Center based on their reporting practice and the lack of chromatographic separation using the method of Van Heukelem and Thomas (2001). Divinyl and monovinyl chlorophylls *b* are partially resolved and are quantified by peak height when divinyl chlorophyll *b* (DVChl *b*) is present. Peridinin (Peri) and phaeophytin *a* (Phytin *a*) include their respective epimers (if detected). Carotene (Caro) represents the sum of β , β -carotene and β , ϵ -carotene. Total Chl *a* (TChl *a*) was used to compute Pig/Chl *a* and C/Chl *a* ratios, which includes the sum of monovinyl Chl *a* or divinyl Chl *a* (DVChl *a*), chlorophyllide *a* and Chl *a* allomers and epimers as defined in Hooker et al. (2005).

TABLE 1. Phytoplankton strain numbers (CCMP = Provasoli-Guillard National Center for Culture of Marine Phytoplankton), names, growth temperature, size (in units of biovolume), growth rate (μ), doubling time (Td), and major/minor axes (μm) for all 43 species (51 strains) examined, grouped by class.

Strain number	Strain name	Temp (°C)	ExpP (μm ³)	StatP (μm ³)	μ (d ⁻¹)	Td (d)	ExpP axes (μm)		StatP axes (μm)	
							Maj.	Min.	Maj.	Min.
Diatoms										
127	<i>Amphora coffeaeformis</i>	14	508.7	1,105.3	0.30	2.31	18	6	22	8
3261	<i>Chaetoceros diadema</i>	14	452.2	—	0.42	1.65	16	6	—	—
1316	<i>Chaetoceros muelleri</i>	24	307.7	502.4	0.40	1.73	8	7	10	8
3263	<i>Chaetoceros socialis</i>	20	282.6	339.1	0.27	2.57	10	6	12	6
308	<i>Corethron hystrix</i>	20	41,849.9	—	—	—	68	28	—	—
359	<i>Ditylum brightwellii</i>	20	31,086.0	—	0.24	2.86	99	20	—	—
2227	<i>Ditylum brightwellii</i>	20	31,028.0	—	1.96	0.35	98	20	—	—
3369	<i>Ditylum brightwellii</i>	20	24,531.0	—	1.37	0.51	50	25	—	—
3323	<i>Fragilariopsis cylindrus</i>	2	42.4	—	—	—	3.5	5	—	—
1094	<i>Grammonema striatula</i>	2	2,747.5	2,747.5	0.28	2.48	35	20	35	20
580	<i>Nitzschia</i> sp.	2	1,899.7	—	—	—	20	11	—	—
632	<i>Phaeodactylum tricornutum</i>	20	148.4	—	—	—	22	3	—	—
1330	<i>Rhizosolenia setigera</i>	2	31,400	—	—	—	51	28	—	—
988	<i>Thalassiosira guillardii</i>	14	265.3	502.4	0.53	1.31	7	7	10	8
1017	<i>Thalassiosira nordenskiöldii</i>	2	1,130	—	0.25	2.72	22.5	8	—	—
1005	<i>Thalassiosira oceanica</i>	20	402.0	945.0	0.68	1.02	8	8	12	10
				402.0	0.36	1.93				
Chlorarachniophyte										
2755	<i>Bigelowiella natans</i>	24	65.4	113.4	0.50	1.38	5	5	6	6
Cyanobacteria										
3462	<i>Microcystis aeruginosa</i>	20	65.3	—	—	—	5	5	—	—
2389	<i>Prochlorococcus marinus</i>	24	0.1	0.1	0.10	6.93	0.5	0.5	0.5	0.5
1333	<i>Synechococcus bacillaris</i>	24	1.1	1.1	0.36	1.93	1.3	1.3	1.3	1.3
1334	<i>Synechococcus</i> sp.	24	0.5	0.5	0.62	1.12	1	1	1	1
				0.5	0.72	0.96				
1985	<i>Trichodesmium erythraeum</i>	24	282.6	—	—	—	12	6.5	—	—
Cryptophyte										
1319	<i>Rhodomonas salina</i>	24	282.1	434.7	1.01	0.69	11	7	13	8
Dinoflagellates										
119	<i>Amphidinium cartarae</i>	24	1,135	—	0.54	1.28	22	10	—	—
2400	<i>Amphidinium cartarae</i>	20	1,127	—	0.44	1.58	21.5	10	—	—
120	<i>Amphidinium gibbosum</i>	24	8,612	—	—	—	34	22	—	—
1771	<i>Alexandrium tamarense</i>	14	33,493.3	—	—	—	21	20	—	—
445	<i>Heterocapsa arctica</i>	2	835.0	—	—	—	16	10	—	—
2281	<i>Karenia brevis</i>	24	7,598.8	13,129.4	0.52	1.33	30	22	32	28
3310	<i>Prorocentrum lima</i>	20	15,641.9	—	—	—	41	27	—	—
1329	<i>Prorocentrum minimum</i>	24	6,367.4	9,198.1	0.28	2.48	30.5	20	30	24
Pelagophyte										
1756	<i>Pelagomonas calceolata</i>	24	6	13	0.70	1.00	3	2	3	3
Prasinophytes										
3430	<i>Ostreococcus lucimarinus</i>	20	1.1	1.1	0.59	1.17	1.3	1.3	1.3	1.3
				1.1	0.21	3.30				
1194	<i>Prasinococcus capsulatus</i>	20	33.5	65.4	0.35	1.98	4	4	5	5
725	<i>Pyramimonas parkae</i>	24	731.5	836.0	0.28	2.48	14	10	16	10
908	<i>Tetraselmis</i> sp.	24	678	942	0.23	3.01	16	9	18	10
Haptophytes										
3382	<i>Chrysotila stipitata</i>	20	1,436.1	—	0.28	2.48	14	14	—	—
298	<i>Crucioplacolithus neohelis</i>	24	220.8	—	—	—	7	7	—	—
371	<i>Emiliania huxleyi</i>	20	1,436.1	3,052.1	0.43	1.61	14	14	18	18
373	<i>Emiliania huxleyi</i>	20	113	268	0.51	1.36	6	6	8	8
1949	<i>Emiliania huxleyi</i>	14	113	268	0.35	1.98	6	6	8	8
1323	<i>Isochrysis galbana</i>	24	28.3	—	—	—	6	3	—	—
3314	<i>Phaeocystis antarctica</i>	2	4.2	14.1	0.71	0.98	2	2	3	3
1805	<i>Phaeocystis globosa</i>	14	113	2,143.6	0.53	1.31	6	6	16	16
647	<i>Pleurochrysis carterae</i>	14	1,149.8	3,589.5	0.58	1.20	13	13	21.2	18
708	<i>Prymnesium parvum</i>	14	368.4	—	—	—	9	8	—	—
1757	<i>Prymnesium polyplepis</i>	14	179.2	179.2	0.69	1.00	7	7	7	7
Raphidophytes										
452	<i>Heterosigma akashiwo</i>	20	977.0	—	0.57	1.22	7	6	—	—
1680	<i>Heterosigma akashiwo</i>	14	1,841.0	—	0.63	1.10	18	14	—	—
2393	<i>Heterosigma akashiwo</i>	14	1,588.0	—	0.58	1.19	15	14	—	—
3374	<i>Heterosigma akashiwo</i>	14	996.0	—	0.64	1.08	7	6	—	—

Values in bold represent results from the climate change treatment.

ExpP, exponential phase; StatP, stationary phase.

TABLE 2. Chromatographic and optical properties of phytoplankton pigments measured in this study in order of retention time in units of minutes (min) and absorption in units of nanometers (nm).

No	Pigment	Abbreviation	Retention time (min)	Absorption maxima (nm)
1	Chlorophyll c_3	Chl c_3	3.7	456, 588, (626)
2	Chlorophyll c_2	Chl c_2	5.9	446, 584, 634
	Chlorophyll c_1		6.2	442, 580, 632
3	Chlorophyllide a	Chlide a	6.3	(380), 434, 620, 666
4	Pheophorbide a	Phide a	8.1	410, 508, 538, 610, 666
5	Peridinin	Peri	10.0	476
6	19' Butanoyloxyfucoxanthin	But	13.6	448, 468
7	Fucoxanthin	Fuco	14.0	452
8	Loroxanthin-like	Loro	14.9	(422), 446, 474
9	Neoxanthin	Neo	15.1	412, 436, 464
10	Prasinoxanthin	Pras	15.3	458
11	Violaxanthin	Viola	15.6	416, 440, 468
12	19' Hexanoyloxyfucoxanthin	Hex	15.9	446, 468
13	Diadinoxanthin	Diad	17.2	(424), 446, 474
14	Alloxanthin	Allo	18.7	(428), 450, 480
15	Diatoxanthin	Diato	19.5	(428), 450, 478
16	Zeaxanthin	Zea	20.3	(428), 450, 476
17	Lutein	Lut	20.6	(422), 444, 472
18	Gyroxanthin diester	Gyro	23.4	(424), 444, 470
19	Divinyl Chlorophyll b	DVChl b	25.6	478, 606, 656
20	Monovinyl Chlorophyll b	Chl b	25.7	468, 602, 650
21	Divinyl Chlorophyll a	DVChl a	28.1	(390), 440, 624, 666
22	Monovinyl Chlorophyll a	Chl a	28.3	(388), 432, 618, 666
23	Pheophytin a	Phytin a	30.2	408, 506, 536, 608, 666
	β , ϵ -carotene	Caro	31.2	(422), 444, 472
24	β , β -carotene	Caro	31.3	(428), 452, 476

Parentheses indicate a shoulder.

Quantitation of loroxanthin. A significant but unknown xanthophyll peak was detected in *Tetraselmis* sp., *Pyramimonas parakeae*, and *Bigeloviella natans*. Because a standard was not available, definitive identification and quantitation was not possible, but it was tentatively identified as loroxanthin (Loro), based on (i) a comparison of retention time relative to other known pigments with published chromatograms from the same analysis method, (ii) notation of Loro in literature as a pigment that is “significant but not always present” in chlorophytes (Egeland et al. 1997) and (iii) comparison of spectral wavelength maxima to published literature. Estimates of concentration were calculated for the suspected Loro peak using the calibration factor for lutein (Lut), which has a similar absorption spectrum and was adjusted for molecular weight (Egeland et al. 2011). Loroxanthin either partially or completely coeluted with Neo leading to higher uncertainties for the neoxanthin results. Loroxanthin estimates should be used with caution when comparing any differences between growth phases or species.

Strain differences. To study the potential changes in pigment composition in response to culture adaptation during an extended period of laboratory cultivation, multiple strains of the same species isolated on different historical dates, but from similar geographic regions, were chosen. Two strains of *Amphidinium carterae* were selected for this comparison (Table 1). CCMP119 was isolated in 1985 and CCMP2400 was isolated in 2004, and both strains were isolated from the coastal waters of Florida. Three strains of *Ditylum brightwellii* were compared and included CCMP359, CCMP2227, and CCMP3369, which were isolated from the region around Cape Cod, Massachusetts, USA in 1980, 2001, and 2008, respectively. Four strains of *Heterosigma akashiwo* were selected for this study and included CCMP452, CCMP1680, CCMP2393, and CCMP3374, which were isolated in 1952, 1963, 2002, and 2010, respectively. All *H. akashiwo* strains

were isolated from coastal waters of the US east coast between the states of Rhode Island and Delaware. None of these strains were cryopreserved, and all were continuously cultivated since isolation. Measurements were made during one growth phase only.

Climate change experiment. An experiment was conducted where elevated temperature, pCO₂, and light were used to simulate future oceanic climate change conditions. The species used in this experiment were *Synechococcus* sp. (CCMP1334), *Thalassiosira oceanica* (CCMP1005), and *Ostreococcus lucimarinus* (CCMP3430). The cultures were transitioned to the climate change experimental conditions when they were scaled from 1 to 18 L batch cultures. Both *T. oceanica* and *O. lucimarinus* were grown at 24°C, which was 4°C above the maintenance temperature of 20°C. Owing to incubator limitations, we were unable to grow *Synechococcus* sp. at a temperature higher than its normal maintenance temperature of 24°C. All three strains were grown on a 14:10 h light-dark cycle and at a constant irradiance of ~135 $\mu\text{mol photons} \cdot \text{m}^{-2} \cdot \text{s}^{-1}$; a value ~2.5-fold greater than the maintenance irradiance. All cultures were continuously bubbled with 0.2 μm filtered house air amended with ~0.5% v/v CO₂. Under these conditions, culture pH was reduced to 7.7 compared with 8.1 under maintenance conditions. The cultures were exposed to the climate change conditions for ~10 cell division events prior to bio-optical and biogeochemical measurements. Our choices for the temperature and pH treatments represented the extremes of current climate change projections (Orr et al. 2005, Collins et al. 2013). Note that no direct measurements of CO₂ were made, only pH was determined. pH varied by culture and day based on biomass demand at the time of measurement but averaged 7.8 ± 0.11 units.

Statistical analyses and growth rate calculations. A series of statistical diagnostics were performed to evaluate the

observed differences in each Chl *a*-normalized pigment between growth phases, treatments, and strains. Prior to the application of a statistical test, Pig/Chl *a* values computed from the replicate filters for both carboys at a single sampling event were combined for each growth phase, treatment, or strain. The Anderson Darling test was used to test for normal distribution of the replicates at an alpha value of 0.05 using the *adtest* function in MATLAB. If all sets of replicates passed this test, then a parametric statistical test was used to evaluate the differences in Pig/Chl *a* values. If either set of replicates failed this test, then a nonparametric statistical test was used. For comparisons between growth phases, either a two-tailed, two-sample *t*-test was performed in Excel or a two-tailed Wilcoxon test was applied using the *ranksum* function in MATLAB. Before a *t*-test was performed, an F-test was used to determine whether the variances were equally distributed, and either a two-sample equal variance or a two-sample unequal variance two-tailed *t*-test was used. Similarly, a two-sample *t*-test or a Wilcoxon test was performed to determine whether any of the Pig/Chl *a* ratios were significantly different between strains of *Amphidinium carterae* (CCMP119 and 2400). A one-way analysis of variance (ANOVA) or a Kruskal-Wallis test was used to determine whether any of Pig/Chl *a* ratios were statistically significant ($P < 0.05$) between the strains of *Heterosigma akashiwo* and *Ditylum brightwellii* and to test whether the pigment ratios observed in each species after the climate change experiment were significantly different from those observed in ExpP or StatP. Growth rates (μ) and doubling time (Td) were calculated using the equations in Wood et al. (2005). Mean and standard deviation of Pig/Chl *a*, Pig/C and C/Chl *a* ratios were computed using replicate filters collected from both 25 L carboys and are reported here.

Pig/C was computed using the mean POC and the mean of the pigment concentration from each growth phase, treatment, or strain. The errors associated with the separate analytical measurements of the HPLC pigments and POC were propagated to Pig/C and C/Chl *a* using standard error propagation theory (Holmes and Buhr 2007). The standard deviation of each average ratio was approximated using the equation:

$$\sigma_R \cong \frac{\mu_X}{\mu_Y} \sqrt{CV_X^2 + CV_Y^2 + 3CV_Y^2 CV_X^2 + 8CV_Y^4} \quad (1)$$

where σ_R is the standard deviation of the ratio, μ_X and μ_Y are the average values of the pigment and carbon, respectively, CV_X is the coefficient of variation of the pigment and CV_Y is the coefficient of variation of the carbon measurement. To test the statistical significance between the Pig/C ratios, a three-sigma limit was applied to set the upper and lower limit of each ratio. If the upper and lower limits of the ratios overlapped, the difference between the values was not considered statistically significant.

RESULTS

The following sections will present the pigments identified in each taxon, dependencies of pigment ratios on growth phase, similarities and differences of pigments and ratios between strains of the same species, and results from the climate change experiment. Pig/Chl *a*, Pig/C, and C/Chl *a* ratios for each taxon are reported in Tables S1–S18 in the Supporting Information and are separated into the appropriate taxonomic categories and pigment-based types (Jeffrey et al. 2011). Pig/cell and C/cell

are reported in Tables S19–S28 in the Supporting Information. Pig/Chl *a*, Pig/C and C/Chl *a* ratios that exhibited statistically significant differences between the two growth phases are marked with a “*” in Figures 1 and 2 as well as Tables S1–S18. Although the proceeding sections will focus on differences observed in the diagnostic pigment ratios, it is important to note that the non-diagnostic and photoprotective pigment ratios of Caro, Diad, Diato, and Viola exhibited consistent differences between the growth phases in many of the species. Figures 1 and 2 show the percent difference of the Pig/Chl *a*, Pig/C, and C/Chl *a* ratios between growth phases are indicated by color, where percent differences are described as an increase (red) or decrease (blue) in StatP relative to the ExpP.

The diatoms. The diatoms were separated into two pigment-based types determined by the absence or presence of chlorophyll-*c3* (Chl *c3*) in Type 1 and Type 2 diatoms, respectively (Jeffrey et al. 2011). The diagnostic pigment fucoxanthin (Fuco) was observed in all the diatoms. Zeaxanthin (Zea) was detected in four diatoms: *Chaetoceros diadema*, *Corethron hystrix*, *Chaetoceros socialis* (ExpP only), and *Ditylum brightwellii* (CCMP2227).

Significant differences in Fuco/Chl *a* between the growth phases were observed for *Chaetoceros muelleri*, *Thalassiosira guillardii*, *T. oceanica*; however, the magnitudes of the differences were small, <6%. For these species, Fuco/Chl *a* was higher in StatP except for *C. socialis*. Zea/Chl *a* was 100% lower in StatP for *C. socialis* (Fig. 1; Table S1). For the Pig/C ratios, the largest and only significant difference was observed in Diato/C, which was up to 27-fold higher in StatP in *A. coffeaeformis* and *T. guillardii* (Fig. 2; Table S2).

Three strains of *Ditylum brightwellii*, CCMP359, CCMP2227, and CCMP3369, were measured for the pigment adaptation study. Zea was only detected in CCMP2227. Fuco/Chl *a* was significantly different between all strains. Some significant differences of up to 2-fold were also observed for Chl *c1c2*/Chl *a*, Caro/Chl *a*, Viola/Chl *a*, and Diato/Chl *a* (Fig. 3A; Table S1). All Pig/C ratios exhibited significant differences between the strains, where CCMP2227 most often different from the other two strains. C/Chl *a* was 2- to 4-fold higher in CCMP2227 than both CCMP359 and CCMP3369, which were not significantly different from each other (Fig. 3B; Table S2). Fuco/C was up to 3.5-fold lower in CCMP2227 than the other strains. Caro/C, Diato/C and Viola/C were up to 4-fold different between the strains.

The chlorarachniophyte. Caro, Zea, Chl *b*, Lut, Neo, Viola, and Loro were detected in *Bigelowiella natans* (Table S3). Both Caro/Chl *a* and Loro/Chl *a* were significantly lower in StatP, but the magnitudes of these differences were low ($\leq 5\%$; Fig. 1; Table S3). The remaining Pig/Chl *a* ratios were not significantly different between the growth phases. None of

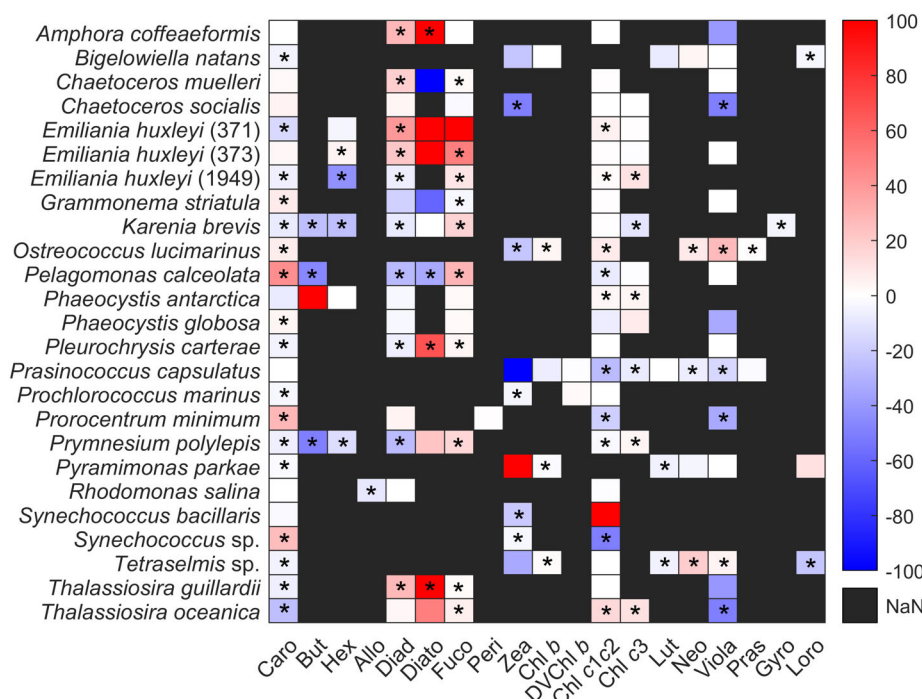


FIG. 1. Heatmap illustrates the percent change of Pig/Chl a from ExpP to StatP. Red color indicates an increase from ExpP to StatP while the blue color indicates a decrease. NaN indicates pigments that were not present.

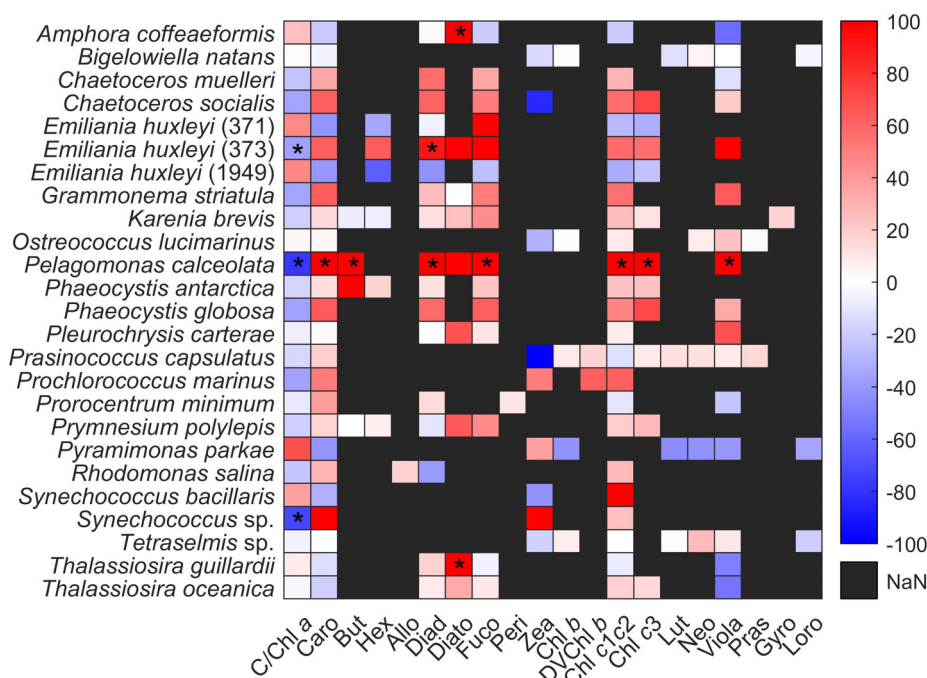


FIG. 2. Heatmap illustrates the percent change of Pig/C from ExpP to StatP. Red color indicates an increase from ExpP to StatP while the blue color indicates a decrease. NaN indicates pigments that were not present.

the Pig/C ratios were determined to be significantly different (Fig. 2; Table S4).

The cyanobacteria. Three pigment-based types of cyanobacteria were measured in this study (Jeffrey et

al. 2011). Caro, Zea and Chl c1c2 were detected in the Type 1 cyanobacterium *Trichodesmium erythraeum* and Type 2 cyanobacteria *Synechococcus bacillaris* and *Synechococcus* sp. (Table S5). For *S. bacillaris*, Chl

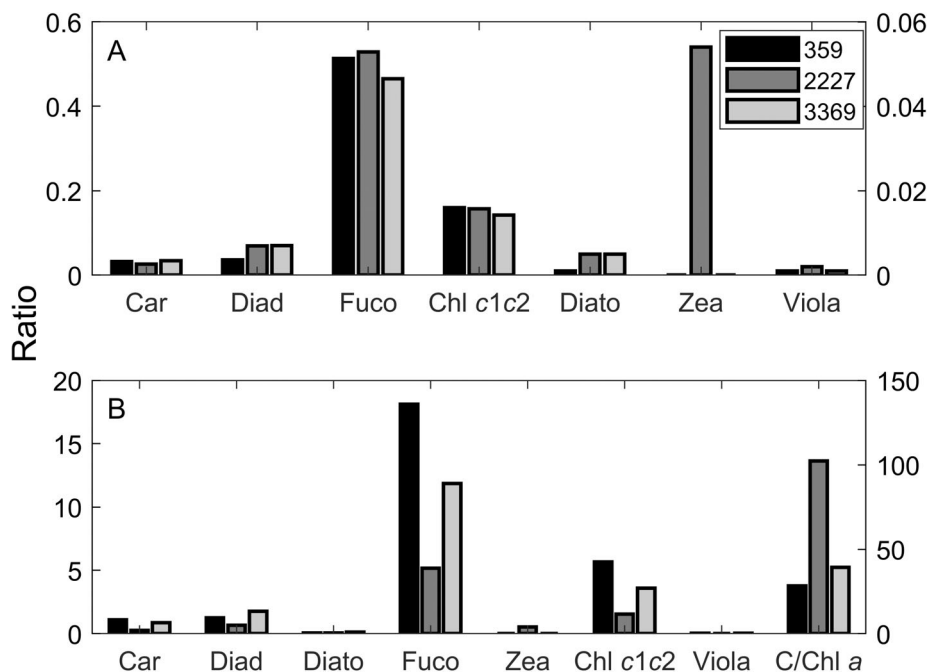


FIG. 3. (A) Pig/Chl *a* (unitless) and (B) Pig/C ($\mu\text{g} \cdot \text{mg}^{-1}$) values for the three strains of *Ditylum brightwellii*. The right y-axes represent the scale for Diato/Chl *a*, Zea/Chl *a*, Viola/Chl *a*, and C/Chl *a*. The left y-axis represents the scale for all other pigments.

c1c2 was only detected in StatP. *Prochlorococcus marinus*, a Type 4 cyanobacteria species, expressed divinyl DVChl *a*, DVChl *b*, Caro, and a trace amount of Chl *c1c2*. Lastly, *Microcystis aeruginosa*, which is not categorized as a specific pigment-based type, expressed the pigments Caro, Zea and Chl *a*. Zea is considered a diagnostic pigment for cyanobacteria, while the presence of both DVChl *b* and DVChl *a* is considered an indicator for *Prochlorococcus* species. For *S. bacillaris* Zea/Chl *a* was 21% lower in StatP (Fig. 1; Table S5). Zea/Chl *a* was also significantly lower in StatP for *Synechococcus* sp. and *P. marinus* but at a lower magnitude ($\leq 4\%$). In *Synechococcus* sp., C/Chl *a* was 71% lower in StatP (Fig. 2; Table S6). Although some minor differences were observed between the growth phases, none of the Pig/C ratios were considered significantly different in *P. marinus* or *S. bacillaris*.

The cryptophyte. Four pigments were detected in the cryptophyte *Rhodomonas salina*: Caro, Diad, alloxanthin (Allo), and Chl *c1c2*. Allo is a diagnostic pigment for cryptophytes. Diato was not detected during either growth phase. Only Allo/Chl *a* was significantly different between the growth phases and was 9% lower in StatP (Fig. 1; Table S7). Although some minor differences were observed between the growth phases, none of the Pig/C ratios were found to be significantly different (Fig. 2; Table S8).

The dinoflagellates. Two dinoflagellate pigment-based types were measured during the experiments (Carreto et al. 2001, Jeffrey et al. 2011). Peridinin

(Peri) is a diagnostic pigment for Type 1 dinoflagellates, while type 2 dinoflagellates like *Karenia brevis* express 19' butanoyloxyfucoxanthin (But), 19' hexanoyloxyfucoxanthin (Hex), Fuco, and Chl *c3*. Additionally, *K. brevis* expresses the diagnostic pigment gyroxanthin diester (Gyro).

For *Karenia brevis*, But/Chl *a*, Hex/Chl *a*, Chl *c3*/Chl *a*, and Gyro/Chl *a* were $\leq 25\%$ lower in StatP (Fig. 1), while Fuco/Chl *a* was 17% higher in StatP. Caro/Chl *a*, Chl *c1c2*/Chl *a*, and Viol/Chl *a* exhibited the largest differences in *Prorocentrum minimum* (Fig. 1; Table S9). Although some differences were observed, none of the Pig/C ratios were determined to be significantly different between the growth phases (Fig. 2; Table S10). All the Pig/Chl *a* ratios were significantly different between the two strains of *Amphidinium carterae* and were generally higher in CCMP2400 (Fig. 4A; Table S9). None of the Pig/C ratios were determined to be significantly different between the two strains (Fig. 4B; Table S10).

The pelagophyte. Eight pigments were detected in the pelagophyte *Pelagomonas calceolata*: Caro, But, Diad, Diato, Fuco, Chl *c1c2*, Chl *c3*, and Viola. For *P. calceolata*, all Pig/Chl *a* ratios were significantly different between the growth phases except for Chl *c3* and Viola (Fig. 1; Table S11). Fuco/Chl *a* and Caro/Chl *a* were up to 44% higher in StatP, while the remaining ratios were lower in StatP by up to 46% (Fig. 1). All Pig/C ratios except Diato/C were significantly different and were ~ 2 to 6-fold higher in StatP. C/Chl *a* was 4.5-fold lower in StatP (Fig. 2; Table S12).

The prasinophytes. Two pigment-based types of prasinophytes were measured in this study (Egeland et al. 1997, Garrido et al. 2009, Jeffrey et al. 2011). Lut, Neo, Zea, Chl *b*, and Loro were detected in the Type 2 prasinophytes (*Pyramimonas parkae* and *Tetraselmis* sp.). Similar pigments were detected in the Type 3 prasinophytes (*Prasinococcus capsulatus* and *Ostreococcus lucimarinus*) with the addition of Pras, a diagnostic pigment for these prasinophyte species. Interestingly, DVChl *b*, which is primarily found in the cyanobacterium *Prochlorococcus*, was detected in *P. capsulatus*. Chl *b* and a Chl *c3*-like pigment were also detected in *P. capsulatus*. In *P. capsulatus*, Zea was only detected during ExpP.

In *Ostreococcus lucimarinus*, all the Pig/Chl *a* ratios were significantly higher in StatP by up to 26% except Zea/Chl *a*, which was 22% lower in StatP. (Fig. 1; Table S13). In *Pyramimonas parkae*, Chl *b*/Chl *a* and Lut/Chl *a* were significantly lower in StatP by $\leq 5.6\%$. In *Prasinococcus capsulatus*, Chl *c3*/Chl *a* was $\sim 8\%$ lower in StatP. For *Tetraselmis* the largest difference was observed for Loro/Chl *a*, which was 22% lower in StatP. Lut/Chl *a* and Chl *b*/Chl *a* were also significantly different between the growth phases but at a much lower magnitude ($\leq 5.7\%$). None of the Pig/C ratios were found to be significantly different between the growth phases (Fig. 2; Table S14).

The haptophytes. Five different haptophyte pigment-based types were measured in this study (Zapata et al. 2004, Jeffrey et al. 2011). Generally, the same pigments were detected in all the haptophytes except for But and Hex, which when present

together are considered diagnostic pigments for Type 6 and 8 haptophytes. But was only detected in *Prymnesium polylepis*, *Phaeocystis antarctica* and the stock (undiluted) culture of *Emiliania huxleyi* (CCMP373; data not shown). Hex was detected in all three strains of *E. huxleyi*, as well as *P. polylepis*, *P. antarctica*.

In *Emiliania huxleyi* (CCMP371), Fuco/Chl *a* was 5.5-fold higher in StatP (Fig. 1; Table S15). For *E. huxleyi* (CCMP373), Hex/Chl *a* and Fuco/Chl *a* were significantly higher in StatP by up to 50%. In *E. huxleyi* (CCMP1949), all Pig/Chl *a* ratios were significantly different, with Hex/Chl *a* exhibiting the largest difference of 43% lower in StatP. In *Phaeocystis antarctica*, only Caro/Chl *a* was significantly different between the growth phases. For *Phaeocystis globosa*, Chl *c3*/Chl *a* was 7.8% higher in StatP. For *Pleurochrysis carterae* Fuco/Chl *a* was 3.5% lower higher in StatP. In *Prymnesium polylepis*, all ratios were significantly different except for Diato/Chl *a*, where Chl *c3*/Chl *a* and Fuco/Chl *a* were 4% and $\sim 16\%$ higher in StatP, respectively. In *E. huxleyi* (CCMP373) C/Chl *a* was 36% lower in StatP, and Diad/C was ~ 2 -fold higher in StatP (Fig. 2; Table S16). The remaining Pig/C ratios were not significantly different between the growth phases.

When comparing Pig/Chl *a* among the three strains of *Emiliania huxleyi*, Chl *c3*/Chl *a* was similar between the strains (Table S15). Fuco/Chl *a* was lowest in CCMP371 and CCMP373 and was ~ 25 -fold higher in CCMP1949. Hex/Chl *a* was ~ 10 -fold higher in CCMP371 and CCMP373 compared to CCMP1949. Like Chl *c3*/Chl *a*, Chl *c3*/C was similar

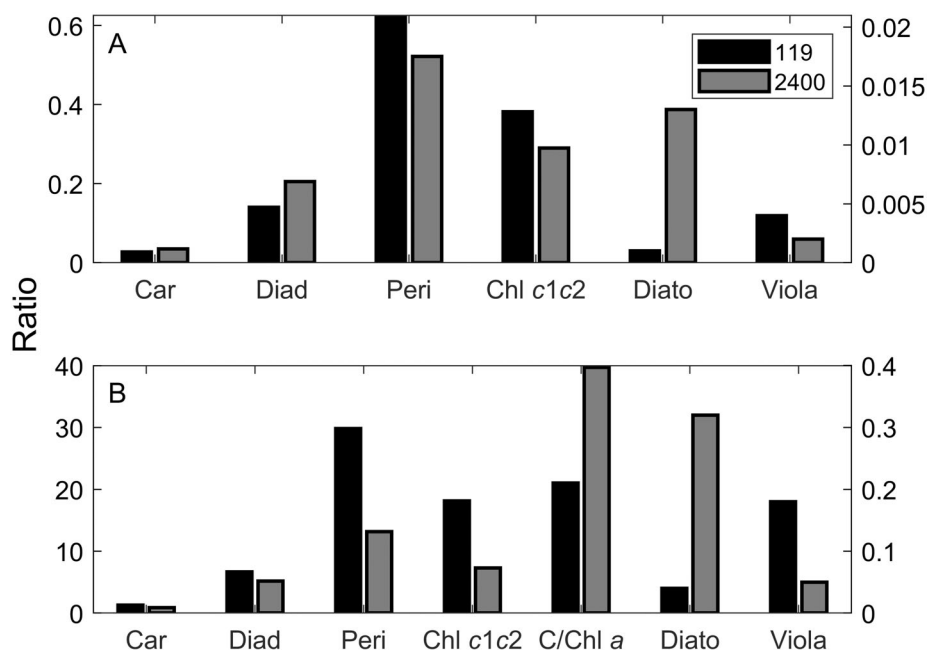


FIG. 4. (A) Pig/Chl *a* (unitless) and (B) Pig/C ($\mu\text{g} \cdot \text{mg}^{-1}$) values for the two strains of *Amphidinium carterae*. The right y-axes represent the scale for Diato/Chl *a* and Viola/Chl *a*. The left y-axis represents the scale for all other pigments.

among the strains. Fuco/C was ~40-fold higher in CCMP1949 than in CCMP371 and CCMP373, and Hex/C was ~10-fold higher in CCMP371 and CCMP373 than CCMP1949 (Table S16).

The raphidophytes. Five pigments were detected in the four strains of *Heterosigma akashiwo*: Caro, Fuco, Zea, Chl *c1c2*, and Viola. For Fuco/Chl *a*, values observed for CCMP452 and CCMP1680 were 4% and 9% higher than CCMP3374, respectively. Fuco/Chl *a* in CCMP2393 was 8% lower than CCMP1680 (Fig. 5A; Table S17). Fuco/Chl *a* was highest in CCMP1680. Zea/Chl *a* in CCMP2393 and CCMP3374 were ~2-fold higher than CCMP1680 and CCMP452. C/Chl *a* in CCMP2393 and CCMP3374 was ~30% higher than CCMP452 and CCMP1680 (Fig. 5B; Table S18). Fuco/C in CCMP3374 and CCMP2393 was ~34% lower than CCMP1680 and CCMP452. Zea/C in CCMP452 was 45% lower than CCMP2393.

Climate change study results. In *Ostreococcus lucimarinus*, Chl *b*/Chl *a* was 4% lower than StatP. Pras/Chl *a* was 5%–6% higher than ExpP and StatP (Fig. 6A). Zea was not detected in the CC-treated culture. Viola/Chl *a* was up to 39% lower than ExpP and StatP. C · cell⁻¹ and C · μm⁻³ were less than half those measured in either ExpP or StatP (Table S28). C/Chl *a* in the CC-treated culture was 6-fold higher than in either growth phase (Fig. 6B; Table S13). The remaining Pig/C ratios were up to 9-fold lower than in ExpP and StatP.

For *Synechococcus* sp., Chl *b*-like, Neo-like and Viola-like pigments were observed in the CC-treated

culture (Fig. 7A; Table S5). Caro/Chl *a* in the CC treatment fell between the values measured in ExpP and StatP. Zea/Chl *a* was 3% lower than in ExpP but the same value as in StatP. C/cell and C/μm³ were up to 24-fold lower than during either ExpP or StatP (Table S28). None of the Pig/C ratios measured after the CC treatment were significantly different than those observed in ExpP or StatP (Fig. 7B; Table S6).

For *Thalassiosira oceanica*, Fuco/Chl *a* was 6% higher than in ExpP but similar to StatP. Chl *c3*/Chl *a* was 58% higher than in ExpP and 41% higher than StatP (Fig. 8A; Table S1). Chl *c1c2*/Chl *a* was up to 19% lower and Diad/Chl *a* was 9% higher than ExpP and StatP, respectively. The largest differences between the CC-treated culture and the maintenance cultures were observed in the carbon measurements. C/cell and C · μm⁻³ were 18% higher than in ExpP and 24% to 3-fold lower than in StatP (Table S28). C/Chl *a* was ~20-fold higher than in ExpP and StatP (Fig. 8B; Table S2). Fuco/C was ~20-fold lower than in ExpP and StatP. Chl *c3*/C was up to 14-fold lower than in ExpP and StatP. The remaining Pig/C ratios were up to 20-fold different than the maintenance cultures.

Comparison of shared diagnostic pigments between groups. The diagnostic pigments shared between different taxonomic groups include But, Chl *b*, Chl *c3*, DVChl *b*, Fuco, Hex, and Zea. This section will focus on comparing these shared Pig/Chl *a* and Pig/C ratios between taxonomic groups. For these comparisons, the average pigment ratios and

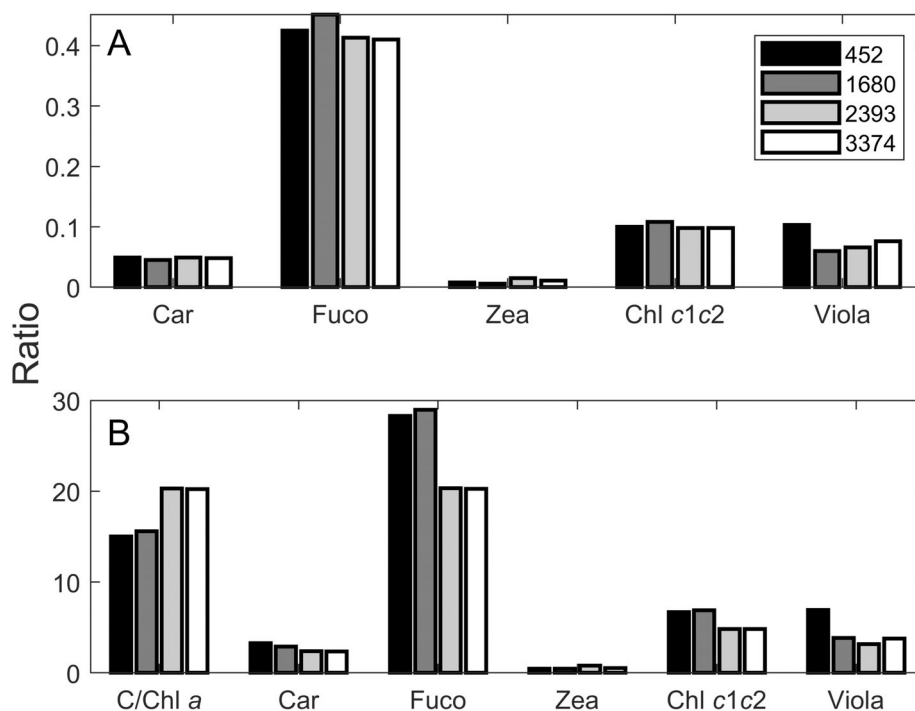


FIG. 5. (A) Pig/Chl *a* (unitless) and (B) Pig/C (μg · mg⁻¹) values for the four strains of *Heterosigma akashiwo*.

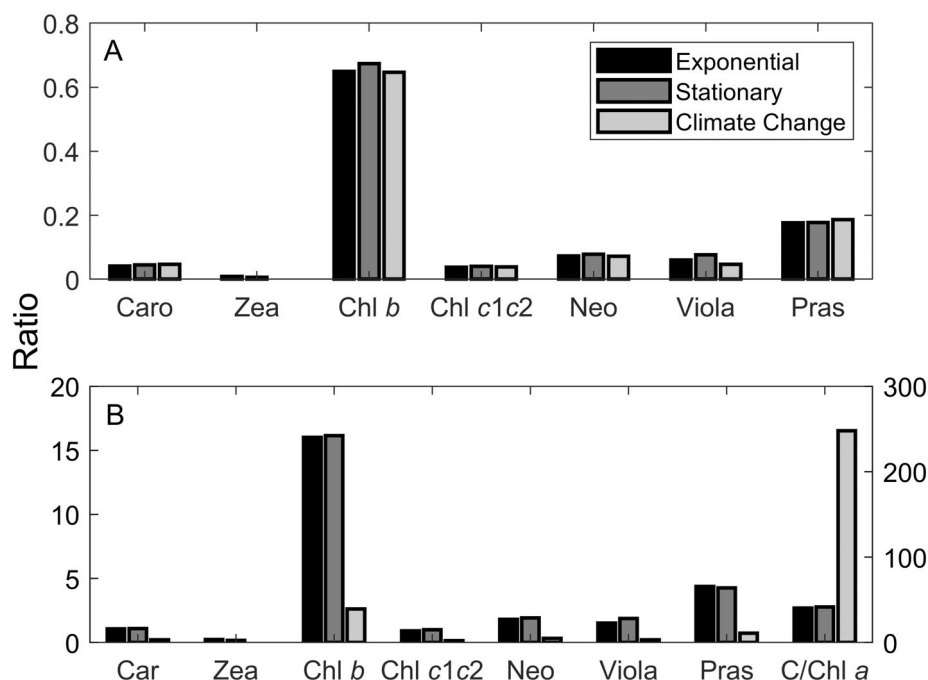


FIG. 6. (A) Pig/Chl *a* (unitless) and (B) Pig/C ($\mu\text{g} \cdot \text{mg}^{-1}$) values for *Ostreococcus lucimarinus* from the maintenance (ExpP and StatP) and the climate change treatment. The right y-axis in panel B represents the scale for C/Chl *a*. The left y-axis represents the scale for all other pigments.

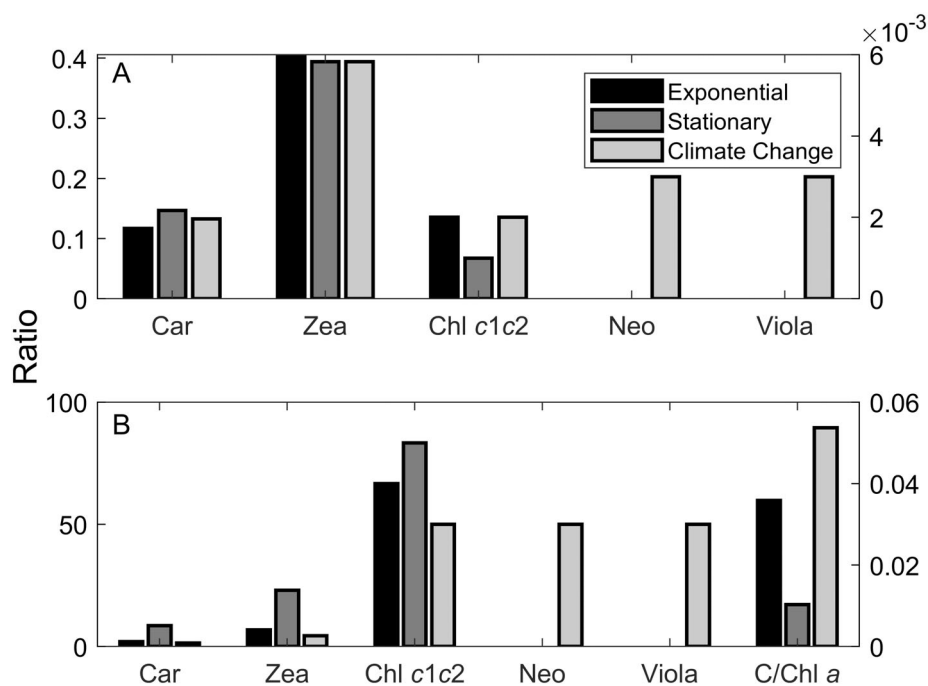


FIG. 7. (A) Pig/Chl *a* (unitless) and (B) Pig/C ($\mu\text{g} \cdot \text{mg}^{-1}$) values for *Synechococcus* sp. from the maintenance (ExpP and StatP) and the climate change treatment. The right y-axes represent the scale for Chl *c1c2*/Chl *a*, Neo/Chl *a* and Viola/Chl *a*. The left y-axis represents the scale for all other pigments.

biovolume from both growth phases were computed. For Figures S1–S7 in the Supporting Information, bubble color indicates higher taxonomic

group and bubble diameter is indicative of comparative biovolume between the taxa. For all the comparisons, it may be noted that there is no apparent

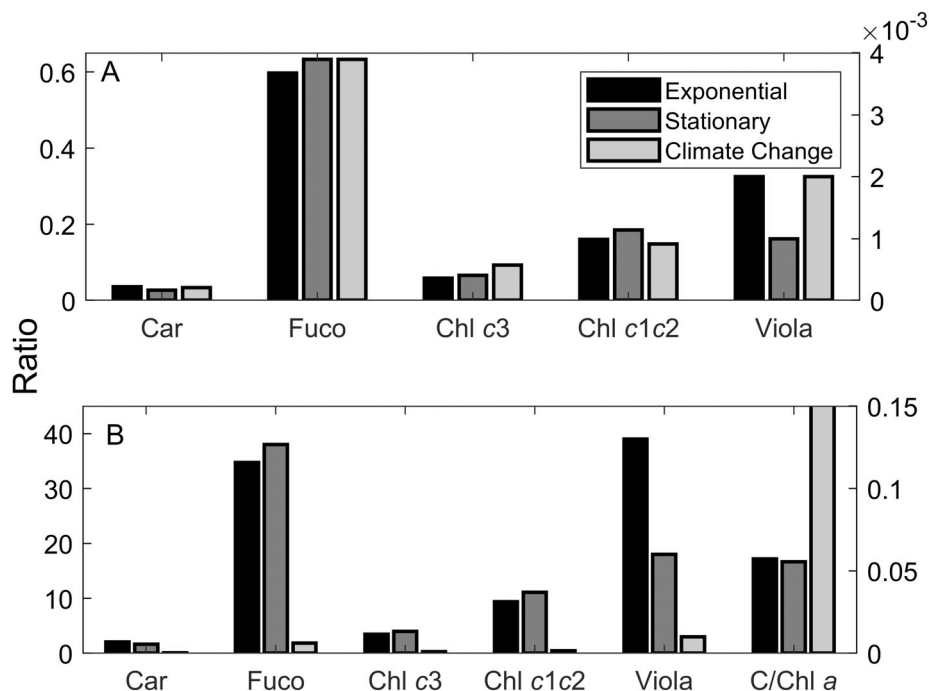


FIG. 8. (A) Pig/Chl *a* (unitless) and (B) Pig/C ($\mu\text{g} \cdot \text{mg}^{-1}$) values for *Thalassiosira oceanica* from the maintenance (ExpP and StatP) and the climate change treatment. The right y-axes represent the scale for Viola/Chl *a*. The left y-axis represents the scale for all other pigments.

trend between cell size and the pigment ratios, meaning that the overlap in pigment ratios between groups occurs despite some observed large differences in cell size. Firstly, But was shared among the dinoflagellate *Karenia brevis*, the pelagophyte *Pelagomonas calceolata* and the haptophytes *Phaeocystis antarctica* and *Prymnesium polylepis*. But/Chl *a* in *P. calceolata* was 10-fold higher than *K. brevis* and over 100-fold higher than *P. antarctica* and *P. polylepis*, which expressed the lowest values (Fig. S1A). But/C was different among the three groups, with the highest ratio observed in *P. calceolata*, which was 3.5-fold higher than *K. brevis* and up to 200-fold higher than *P. antarctica* and *P. polylepis* (Fig. S1B).

Chl *b* was shared between *Bigelowiella natans* and all prasinophytes in this study. Chl *b*/Chl *a* in *B. natans* was up to ~40% higher than *Pyramimonas parkae*, *Tetraselmis* sp., and *Ostreococcus lucimarinus* and 7-fold higher than *Prasinococcus capsulatus* (Fig. S2A). Chl *b*/C in *B. natans* was similar to *P. parkae* and *Tetraselmis* sp. but was 2 and 15-fold higher than *O. lucimarinus* and *P. capsulatus*, respectively (Fig. S2B).

Chl *c3* was shared between Type 2 diatoms, *Karenia brevis*, *Pelagomonas calceolata*, *Prasinococcus capsulatus*, and all haptophytes except *Chrysotila stipitata*. The average Chl *c3*/Chl *a* and Chl *c3*/C ratios among the groups largely overlapped and varied greatly depending on species. Some of the lowest values of Chl *c3*/Chl *a* and Chl *c3*/C were observed in *P. capsulatus*, *Phaeocystis antarctica*, *Cruciplacolithus*

neohelis and the Type 2 diatoms except for *Chaetoceros diadema* (Fig. S3). The highest values of Chl *c3*/Chl *a* and Chl *c3*/C were observed in *P. globosa*, which were up to 180-fold and 800-fold higher, respectively, than the other taxa (Fig. S3A). Chl *c3*/Chl *a* in *P. calceolata* was similar to most of the haptophytes but was up to 3-fold higher than *C. neohelis*, *Prymnesium parvum*, and *P. antarctica*. Chl *c3*/Chl *a* in *K. brevis* was similar to *C. neohelis*, *P. parvum* and *P. antarctica*. Average values of Chl *c3*/C were similar between *K. brevis*, *P. calceolata*, and most of the haptophytes except for *P. globosa* and *P. antarctica* (Fig. S3B). Type 2 diatoms exhibited some of the lowest Chl *c3*/C ratios.

DVChl *b* was observed in two groups during this study: *Prasinococcus capsulatus* and *Prochlorococcus marinus*. DVChl *b*/Chl *a* was 6-fold higher in *P. capsulatus* than *P. marinus* (Fig. S4A). Average DVChl *b*/C was 2-fold higher in *P. capsulatus* than *P. marinus* (Fig. S4B). *Prochlorococcus marinus* also expressed DVChl *a*, which was not observed in *P. capsulatus*. The presence or absence of DVChl *a*, which is also a diagnostic pigment for *Prochlorococcus* species, in addition to the large difference between DVChl *b* ratios, should distinguish the two species.

Fuco was a shared pigment among all diatoms, *Karenia brevis*, *Pelagomonas calceolata*, all haptophytes, and all strains of *Heterosigma akashiwo*. A trace amount of a Fuco-like pigment was observed in the cyanobacterium *Trichodesmium erythraeum* (not included in Fig. S5). Values of Fuco/Chl *a* in the

diatoms were similar to each other, ranging from 0.340 to 0.662 (Fig. S5A). *Pelagomonas calceolata* exhibited Fuco/Chl *a* ratios at the higher end of the range observed in the diatoms, while the raphidophyte ratios fell within the middle of the range. Average Fuco/Chl *a* in *K. brevis* was below the range the diatoms but within range of the haptophytes. Fuco/Chl *a* in the haptophytes varied considerably, with most ratios falling into the range of the diatoms, while *Emiliania huxleyi* (CCMP1949) and *Phaeocystis globosa* exceeded the highest Fuco/Chl *a* in *C. hystrix* by ~30%. Fuco/Chl *a* in *T. erythraeum* was much lower than all other groups. The second lowest Fuco/Chl *a* values were observed in *E. huxleyi* (CCMP371/373), up to 50-fold lower than the diatoms. Values of Fuco/Chl *a* observed for the *H. akashiwo* were similar to *Chaetoceros diadema* and *C. muelleri*. *Karenia brevis* exhibited Fuco/Chl *a* values like many of the haptophytes, particularly *Prymnesium polylepis* and *Isochrysis galbana*. Fuco/C among the groups was even more variable than Fuco/Chl *a* (Fig. S5B). *Phaeocystis globosa* exhibited the highest Fuco/C ratio, up to 10-fold higher than the diatoms, while the diatoms were up to 20-fold higher than the haptophyte *Phaeocystis antarctica*. The lowest Fuco/C was observed in *E. huxleyi* (CCMP371/373), which was up to 200-fold lower than the diatoms.

19' Hexanoyloxyfucoxanthin(Hex) was shared among the haptophytes and *Karenia brevis*. Hex/Chl *a* was up to 50-fold higher in the haptophytes than in *K. brevis* (Fig. S6A). For Hex/C, the haptophytes, except *Phaeocystis antarctica* were 2- to 19-fold higher than *K. brevis*, while *P. antarctica* was almost 15% lower than *K. brevis* (Fig. S6B).

Zea was a shared pigment among *Bigelowiella natans*, the cyanophytes, Type 2 diatoms, one strain of *Ditylum brightwellii* (CCMP2227), the prasinophytes and the raphidophytes. Zea/Chl *a* was up to ~88-fold higher in the cyanophytes than the other taxa (Fig. S7A). Values of Zea/Chl *a* in the non-cyanophytes were low and similar to each other. Average Zea/C in the cyanophytes was up to ~100-fold higher than the diatoms and ~20–300-fold higher than the other taxa (Fig. S7B).

DISCUSSION

The pigment composition of 51 phytoplankton strains were measured in this study, covering most major phytoplankton groups and included representatives of both coastal and open ocean environments. Most of the diagnostic pigments observed in this study met expectations with a few interesting observations. DVChl *b*, a known diagnostic pigment for *Prochlorococcus marinus* (Chisholm et al. 1992) was observed in the prasinophyte *Prasinococcus capsulatus*, which has not been previously reported. We also estimated values for a pigment presumed to be Loro, which coelutes with Neo (with this analysis method) and is unique to prasinophytes,

particularly *Tetraselmis* sp., (Fawley 1991, Garrido et al. 2009) and was also observed in *Bigelowiella natans*.

Extensive literature review of either the same or similar species observed in this study showed that large ranges of Pig/Chl *a* values exist for each taxonomic group. The Pig/Chl *a* values observed in this study generally fell within the wide range in values for diatoms (Sakshaug et al. 1991, Schlüter et al. 2000, Henriksen et al. 2002), dinoflagellates (Schlüter et al. 2000, Seoane et al. 2006, Ruivo et al. 2011, Liu et al. 2014, Clementson and Wojtasiewicz 2019), cyanobacteria (Moore et al. 1995, Schlüter et al. 2000, DiTullio et al. 2005, MacIntyre and Cullen 2005), cryptophytes (Schlüter et al. 2000, Henriksen et al. 2002, Ruivo et al. 2011), pelagophytes (Schlüter et al. 2000, Dimier et al. 2009), prasinophytes (Schlüter et al. 2000, Latasa et al. 2004, Laza-Martinez et al. 2007, Clementson and Wojtasiewicz 2019), haptophytes (Schlüter et al. 2000, Zapata et al. 2004, Laza-Martinez et al. 2007), and the raphidophyte *Heterosigma akashiwo* (Seoane et al. 2006, Laza-Martinez et al. 2007). However, there were a few exceptions. For example, the values of Chl *b*/Chl *a* in *Prasinococcus capsulatus* and Zea/Chl *a* in *Ostreococcus lucimarinus* in this study were 78% and up to 90% lower, respectively, than the literature values of similar species (Latasa et al. 2004). However, with regard to Chl *b*/Chl *a* in *P. capsulatus*, it should be noted that the Zapata et al. (2000) method implemented in Latasa et al. (2004) does not completely separate Chl *b* from DVChl *b*. It is possible that Chl *b* concentrations reported in Latasa et al. (2004) could be the sum of Chl *b* and DVChl *b*, which would explain the higher values of Chl *b*/Chl *a*. Hex/Chl *a* in *Emiliania huxleyi* (CCMP1949) was up to 97% lower than the values for various strains of *E. huxleyi* in the literature (Schlüter et al. 2000, Zapata et al. 2004, Seoane et al. 2006). Chl *c3*/Chl *a* in *Prymnesium parvum* observed during this study was up to 9% higher than values in the literature (Zapata et al. 2004), while Fuco/Chl *a* in *Prymnesium polylepis* was up to 97% higher than literature values (Zapata et al. 2001, Zapata et al. 2004). Fuco/Chl *a* and Chl *c3*/Chl *a* in *Phaeocystis globosa* measured in this study were up to 75% higher than values in the literature (Zapata et al. 2004, Rodriguez et al. 2006, Laza-Martinez et al. 2007). But and Hex were not detected in *P. globosa* (CCMP1805) in this study but have been observed in other strains (Zapata et al. 2004, Rodriguez et al. 2006). Literature values for *Bigelowiella natans* could not be found.

Few studies have reported Pig/C ratios, although a limited number of C/Chl *a* ratios have been reported for various taxonomic groups, particularly for diatoms. Finenko et al. (2003) reported a comprehensive list of literature values for C/Chl *a* in a select number of taxonomic groups. Although many of the values of C/Chl *a* were measured in response

to variations on light availability, we can still get sense of how the values measured in this study compare to others. For example, C/Chl *a* for diatoms in this study were within the range of those found in the literature (Durbin 1977, Richardson et al. 1996, Anning et al. 2000, Finenko et al. 2003, Leonardos and Geider 2004, Arrigo et al. 2010, Spilling et al. 2015). In *Chaetoceros muelleri*, C/Chl *a* ranged from 23.22 to 175.2 depending on nutrient regimes and light intensity in a study by Leonardos and Geider (2004). In Arrigo et al. (2010), *Fragilariopsis cylindrus* C/Chl *a* ranged from 25 to 96 depending on growth irradiance. Literature values of C/Chl *a* for *C. socialis* (22) and *Phaeodactylum tricornutum* (14.8, 14.9) were similar to those observed in this study (Geider et al. 1985, Terry et al. 1985, Finenko et al. 2003). Additional values of C/Chl *a* for similar taxa listed in (Finenko et al. 2003) are comparable with the values observed in this study, while some differed slightly. For example, C/Chl *a* for *Isochrysis galbana* (11.31) in this study was lower than the literature values that ranged from 30 to 39.4. The results from this study have added important value to the number of known C/Chl *a* values for various phytoplankton species.

Effects of growth phase. One major underlying question of this study was whether growth phase has a significant impact on the pigment ratios. If so, those uncertainties should be considered within models and algorithms that use pigment ratios as input. A limited number of significant differences for the Pig/Chl *a* ratios were observed between the growth phases in this study, although most were small (<10%; Fig. 1). The largest increases from ExpP to StatP in all the taxa occurred for the photoprotective pigments Diad, Diato, Zea, and Viola, which has been observed in previous studies (Latasá 1995, Llewellyn and Gibb 2000, Ruivo et al. 2011). Generally, the Pig/Chl *a* ratios of light-harvesting carotenoids (Caro, Chl *c1c2*, Peri, Fuco, Chl *b*) covaried with Chl *a*, but the covariance was not 1:1 because the ratios increased or decreased based on the net increase or decrease of each pigment. Previous studies have shown that an increase in the ratio of light-harvesting carotenoids to Chl *a* from ExpP to StatP may be caused by the larger degradation of Chl *a* from ExpP to StatP owing to nutrient limitation, specifically nitrogen limitation, in StatP (Henriksen et al. 2002, Ruivo et al. 2011). Carotenoids do not contain nitrogen and are less likely to be broken down under nutrient limitation. However, this pattern was species dependent as increases in Chl *a*/cell between ExpP and StatP were observed. Adjustments in the proportion of reaction centers to light-harvesting complexes can also influence fluctuations in cellular pigments (Ruivo et al. 2011).

Only a few species exhibited significant differences in Pig/C between growth phases, and these differences were determined by the coincident adjustments of cellular carbon and pigments

between ExpP and StatP. For approximately half of the strains both $C \cdot cell^{-1}$ and $C \cdot \mu m^{-3}$ were higher in StatP than in ExpP, the remaining strains exhibiting a decline or no change from ExpP to StatP. Those strains that exhibited lower $C \cdot \mu m^{-3}$ were larger in StatP than in ExpP. Higher $C \cdot cell^{-1}$ in StatP compared to ExpP indicates that the cells continued to accumulate carbon even after growth began to slow owing to the onset of nutrient limitation (Liefer et al. 2019). Assuming Redfield ratios, carbon-to-nitrogen (C:N) ratios for some of the strains, such as *Thalassiosira guillardii*, *Emiliania huxleyi* (CCMP371), *Bigelowiella natans*, and *Prorocentrum minimum* did indicate possible mild nutrient limitation at StatP (C:N > 6.6) but not all strains with higher $C \cdot cell^{-1}$ were nutrient limited. C/Chl *a* varied between species and growth phase and was determined by net increases or decreases in cellular carbon and Chl *a*. Previous studies have shown that C/Chl *a* typically increases with nutrient limitation. It would then be expected that higher C/Chl *a* would be observed in StatP coinciding with the degradation of Chl *a* (Harrison et al. 1977, Kiefer and Cullen 1991, Eker-Develi et al. 2006).

For chemotaxonomic applications such as CHEMTAX (Mackey et al. 1996), species are typically grouped within the same higher taxonomic category (e.g., Type 1 or Type 2 diatoms); therefore, the mean and uncertainty of the entire group will be more pertinent to chemotaxonomic applications. To address whether differences between growth phases may impact the uncertainty in chemotaxonomic methods, we compared the variance of the ratios within each group to the within species variance from the growth phases. We observed that the within group variance (the square of the standard deviation) for diagnostic Pig/Chl *a* and Pig/C ratios largely exceeded the within species variance. For example, the variance of within group Fuco/Chl *a* for both Type 1 and Type 2 diatoms was 0.006, while species variance ranged from $7 \cdot 10^{-5}$ to 0.001 in the type 1 diatoms and $1 \cdot 10^{-4}$ and $6 \cdot 10^{-4}$ in the type 2 diatoms. The within species variance of Peri/Chl *a* in *Prorocentrum minimum* was $4 \cdot 10^{-6}$ and $7 \cdot 10^{-5}$ for *Amphidinium carterae* while within group variance was 0.012. Similarly, within group variance of Hex/Chl *a* for both Type 6 and Type 8 haptophytes (including CCMP1949 in the Type 6 haptophytes) was 0.193 and 0.077, respectively, and group variance of Fuco/Chl *a* was 0.173 and 0.098. Within species variance were within the order of 10^{-6} to 0 for Hex/Chl *a* and Fuco/Chl *a*. Similarly, within group variance of Fuco/C of Type 1 and Type 2 diatoms was 172.66 and 144, respectively while within species variance ranged from 0.99 to 180.88 (*Grammonema striatula*). Note that these variances include differences between strains. These results indicate that, at least for species measured in this study, any differences in the pigment ratios between growth phases and strains was outweighed by within group

differences and, therefore, heavier consideration should be given to those grouped ratios from which the average pigment ratios are computed.

Pigment adaptation study. Laboratory phytoplankton cultures have played an indispensable role in our understanding of phytoplankton physiology and ecology. However, some caution should be exercised when comparing laboratory results to what is observed in nature, particularly when we consider that strains cultivated in the laboratory experience genetic processes that lead to trait differences, which include mutation, recombination, genetic drift, inbreeding, and selection (Wood and Leatham 1992, Lakeman et al. 2009). Wood and Leatham (1992) cited several studies as examples, suggesting “significant interclonal” variability occurs in laboratory cultures over time, resulting in differing physiological and biochemical traits than those observed in the natural environment. To this end, we compared Pig/Chl *a* and Pig/C in two strains of the dinoflagellate species *Amphidinium carterae*, three strains of the diatom species *Ditylum brightwellii* and four strains of the raphidophyte *Heterosigma akashiwo* to observe possible pigment differences owing to culture adaptation over a long cultivation period. Some minor differences in the pigment ratios and cell size between the strains were observed. However, no observable trend within the pigment ratios from youngest to oldest strain was observed for *D. brightwellii* or *H. akashiwo*, indicating that age of isolation did not appear to directly impact the pigment ratios. Some differences were observed between the two *A. carterae* strains, indicating possible pigment adaptation. However, the variability of pigment ratios between the different strains is comparable and within range to that which has been observed in other studies that used different strains. For example, Ruivo et al. (2011) observed values of Peri/Chl *a* in another strain of *A. carterae* (IO 17-01) that ranged between 0.554 and 0.625, depending on growth phase. For *H. akashiwo*, three other studies observed Fuco/Chl *a* values between 0.273 and 0.831 (Rodriguez et al. 2006, Seoane et al. 2006, Laza-Martinez et al. 2007). Henriksen et al. (2002) and Schlüter et al. (2000) observed a wide range of Fuco/Chl *a* values in *D. brightwellii*, from 0.171 up to 1.4, depending on growth phase and light level.

Suggestions for chemotaxonomy. Chemotaxonomic methods that derive PCC from pigments is confounded by strain differences within the same species and shared diagnostic pigments between higher level taxonomic groups. While the pigment adaptation study addressed the impact of cultivation time on pigment ratios, the large differences in the pigment ratios between the three strains of *Emiliania huxleyi* may be a result of adaptations to different environments. CCMP1949 was isolated in a coastal, high nutrient environment (Gulf of Maine) while CCMP371 and CCMP373 were isolated in low

nutrient, oceanic environments (Sargasso Sea). The large variations in pigment ratios for all species and groups found in the literature may in part be due to these environmental adaptations. Likewise, shared diagnostic pigments between taxonomic groups are sources of error in chemotaxonomic methods. For Zea, Hex, Chl *b*, and DVChl *b*, the pigment ratios were different enough to distinguish the groups that shared the pigment expression, and the presence or absence of additional diagnostic pigments would largely chemotaxonomically separate the groups. In contrast, Fuco and Chl *c3* ratios between taxa largely overlapped and were at times almost indistinguishable between some of the groups. The presence of Hex and/or But in conjunction with Fuco and Chl *c3* (if present), can help distinguish the diatoms from the haptophytes. To help mitigate both issues when using pigment ratios to model community composition, the species and associated pigments and pigment ratios should reflect the those predicted to be part of the local population, which are largely based on published values from laboratory cultures and field measurements (Lewitus et al. 2005). The choice of strain and associated pigment ratios from the literature is important, and consideration must be made regarding from where a culture was isolated from as it might still reflect genetic adaptations to the natural environment. In Figure 9, we show the location at which each strain measured in this study was collected, where the colors represent the different phytoplankton classes measured during this project. By using such a map, we can make educated decisions on which strains are appropriate for the region of interest.

Climate change experiment. In anticipation of predicted future changes in the ocean, we examined the impact of the combination of elevated light, temperature, and pCO₂ on cellular pigments and carbon on three species. The results reported here may be used to inform models and chemotaxonomic methods that predict community composition of these anticipated physiological changes. The physiological responses to the climate change conditions differed between the three species, largely with respect to growth rates and cellular carbon. *Thalassiosira oceanica* responded to the treatment with growth rates that were 47% lower than in the maintenance cultures while maintaining C · cell⁻¹ and C · μm⁻³ like those observed in ExpP and StatP. We hypothesize that the lower growth rate could have allowed *T. oceanica* to maintain cell size, as well as cellular carbon quota. This lack of response is contrary to those observed by other diatoms that exhibited an increase in growth rates and size with elevated pCO₂ (Groß et al. 2021). However, a compilation of mixed physiological responses from various diatoms species to elevated CO₂ listed in Gao and Campbell (2014) indicate a species-specific response. Although *T. oceanica* was not stimulated

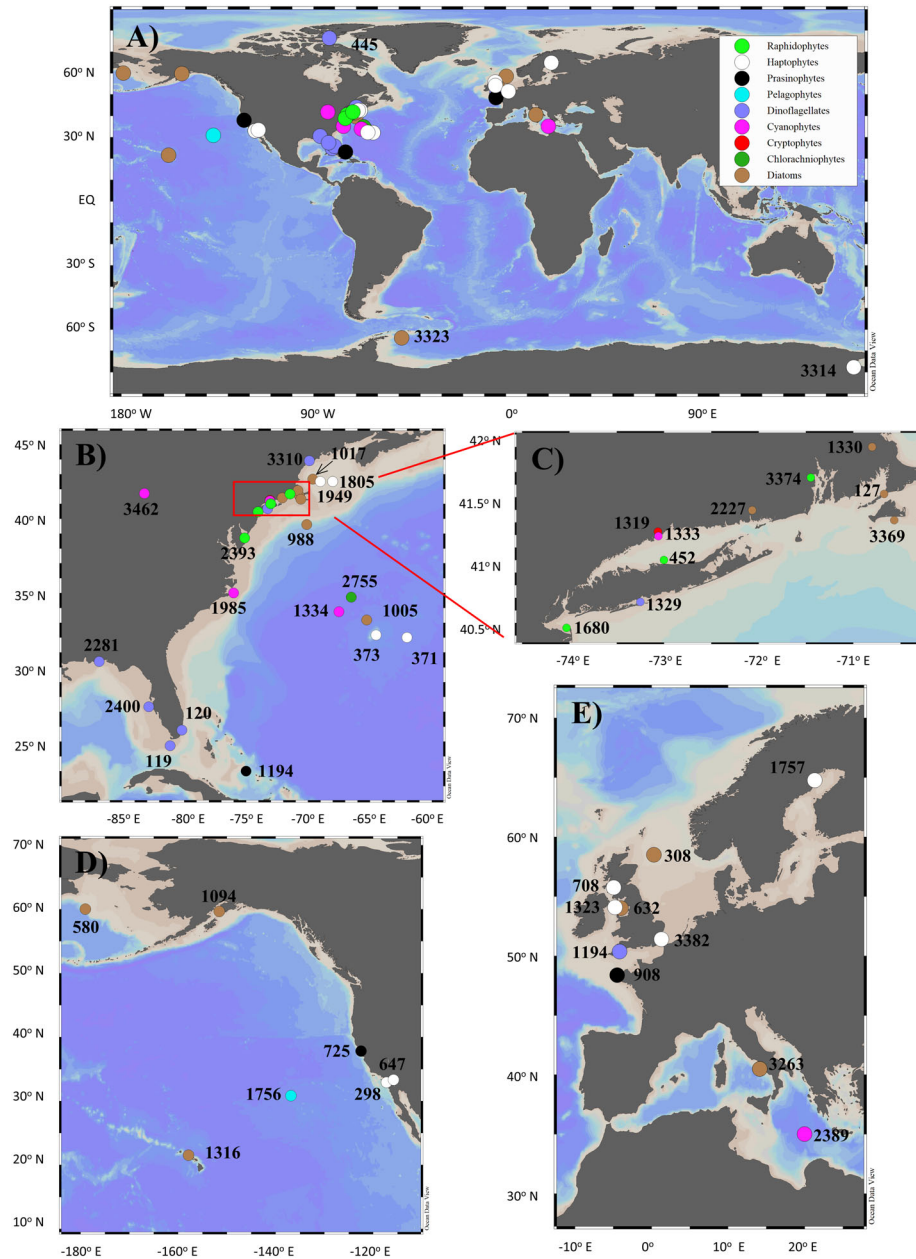


FIG. 9. (A) Map of the global ocean showing the distribution of phytoplankton strains measured in this study. Additional maps focused on specific regions: (B) eastern North Atlantic Ocean and Gulf of Mexico, (C) Baffin Bay, (D) Pacific Ocean, and (E) western North Atlantic Ocean.

by the treatments, growth physiology did not appear to be negatively affected either.

In *Ostreococcus lucimarinus* growth rates were lower than maintenance cultures by 58%, and both $C \cdot cell^{-1}$ and $C \cdot \mu m^{-3}$ were lower under the CC treatment. Growth rates were 15% higher for *Synechococcus* sp. under the CC treatment (light and pH, only) than the maintenance cultures. Like *O. lucimarinus*, both $C/cell$ and $C/\mu m^3$ were lower than the maintenance cultures. For *Synechococcus* sp. a faster growth rate likely led to smaller cells that

have a lower cellular quota for carbon. However, flow cytometry would not necessarily be sensitive enough to capture this small change in cell size. The explanation for the response of *O. lucimarinus* to the treatment is not as straightforward. Cell counts were only collected twice over a 5 d period, including the day on which the culture was harvested. Therefore, it is possible that the log growth period was missed, and the growth rates were higher than calculated here. If this is the case, like *Synechococcus*, higher growth rates could lead to

smaller cells and therefore, lower cellular quotas for carbon. If growth rate was indeed slower during the CC treatment, this would contradict the idea that all small phytoplankton, particularly picoeukaryotes and cyanobacteria will respond positively under a climate change scenario. However, previous studies have shown that the response of different ecotypes of *Ostreococcus* to elevated CO₂, temperature, and light varies and is likely determined by environmental variability and the evolutionary adaptations of each ecotype to that variability, which could explain the response of *O. lucimarinus* to the CC treatment (Schaum et al. 2016). Additionally, Kulk et al. (2012) observed maximum growth rates for *Ostreococcus* sp. between 20 and 24°C. Assuming the strain used in our study is similar to the one in Kulk et al. (2012), it is possible that 24°C was beyond the optimum growth temperature and could explain the possible decline in growth rate observed here.

Generally, the Pig/Chl *a* ratios observed after the CC treatment fell within the range of those observed in ExpP and StatP for *Synechococcus*. Higher values of Chl *c3*/Chl *a* and Pras/Chl *a* and the lower values of Neo/Chl *a* and Viola/Chl *a* were observed in *Thalassiosira oceanica* and *Ostreococcus lucimarinus*. Moreover, a slight increase in Diad/Chl *a* was also observed in *T. oceanica* compared to ExpP and StatP. These observations indicate a possible photochemical response to elevated temperature. Previous studies have shown that phytoplankton respond to elevated temperature by increasing light-harvesting pigments to meet the increase in photosynthesis rates until an optimum temperature is reached (Davison 1991, Thompson et al. 1992, Kulk et al. 2012). Kulk et al. (2012) observed that in *Ostreococcus*, the photoprotective pigment ratios that included the sum of Viola/Chl *a* and Zea/Chl *a* decreased when exposed to elevated temperature. They also observed an increase in But/Chl *a* and Diad+Diat/Chl *a* in *Pelagomonas calceolata* in response to elevated temperature. The short-term photochemical response to elevated temperature may counterbalance photoinhibition from elevated light by dissipating excess thermal energy through the xanthophyll cycle (Demmig-Adams and Adams 1992, Kulk et al. 2012).

The largest differences were observed in Pig/C and C/Chl *a* ratios, where *Thalassiosira oceanica* and *Ostreococcus lucimarinus* exhibited significantly lower Pig/C and higher C/Chl *a* under the CC treatment compared to ExpP and StatP. Neither Pig/C nor C/Chl *a* ratios in *Synechococcus* sp. under the CC treatment were significantly different than those observed in ExpP and StatP. Cellular pigment concentrations were up to 30-fold lower in the CC treatment for all three species, resulting in the higher C/Chl *a* and lower Pig/C values (although not significantly higher in *Synechococcus* sp.), a common adaptation to elevated light known as photoacclimation

(Falkowski and LaRoche 1991). Viola was observed in *Synechococcus* sp. after the CC treatment but was not detected in either ExpP or StatP for, indicating a photoprotective response.

The C:N ratios at the time of culture harvest ranged from 4.34 to 7.38 (data not shown). Assuming the Redfield ratio of ~6.62 for nutrient replete cells, these results indicated that the cultures were not nutrient limited and that the physiologically responses were likely in response to the treatments. Given the results from this multistressor experiment, we may surmise that *Synechococcus* sp. will certainly thrive under environmental conditions influenced by climate change, while it is uncertain for *Thalassiosira oceanica* and *Ostreococcus lucimarinus*. The genus *Synechococcus* generally has an advantage over other species owing to its genetic diversity that allows them to inhabit a broad range of temperature in the global ocean (Mackey et al. 2013). Although the effect of elevated temperature was not tested in this study, other studies have shown that elevated temperature resulted in increased cell division rates in *Synechococcus* (Fu et al. 2007, Mackey et al. 2013).

Consequences for remote sensing applications. Phytoplankton carbon (C-phyto) is a desirable ocean color satellite product that is critical to understanding the global ocean carbon cycle as is C/Chl *a* because it is necessary to derive ocean primary production. Current approaches to derive C-phyto from satellite observations include empirical methods that relate particle backscatter and Chl *a* to C-phyto. Work is underway to develop new approaches that utilize additional inputs, such as in situ C-phyto and biogeochemical parameters. One of NASA's PACE mission core objectives is to understand Earth's Ocean ecosystem through estimates of phytoplankton concentration and community composition as well as ocean productivity. The PACE mission will not only create continuity of biomass estimates through its Chl *a* product, but its complete spectral content, finer spectral resolution and expansion into the ultraviolet spectrum will also improve estimates of phytoplankton pigment concentrations and C-phyto using advanced algorithms. One of the primary objectives of the Phytoplankton Library of Optical Properties and Spectra project was to develop a predictive PCC algorithm using the bio-optical measurements collected from these taxa and to relate the algorithm back to phytoplankton carbon biomass rather than Chl *a*. The pigment ratios, particularly Pig/C, will be used to develop and validate these PCC algorithm(s) by applying a modeling technique that converts the ratios into PCC using methods such as CHEMTAX or Inverse Simultaneous Equations. These advanced data products will be important input variables for ecosystem models and algorithms that aid in fisheries management and detect harmful algal blooms (Werdell et al. 2019). The results from this study will fill a critical need for

globally relevant pigment signatures required for algorithm development and validation activities.

Research was funded by the National Aeronautics and Space Administration Grant # NNX17AB90G. We thank Michael Novak, Grace Kim, and Joan Blanchette for their assistance in sample collection and culture cultivation. The authors have no conflicts of interest to declare.

AUTHOR CONTRIBUTIONS

A.R. Neeley: Conceptualization (lead); data curation (equal); formal analysis (lead); investigation (equal); writing – original draft (lead); writing – review and editing (lead). **M.W. Lomas:** Conceptualization (equal); data curation (equal); formal analysis (supporting); funding acquisition (lead); investigation (lead); project administration (lead); supervision (lead); writing – review and editing (supporting). **A. Mannino:** Conceptualization (equal); data curation (equal); formal analysis (supporting); funding acquisition (lead); investigation (lead); project administration (lead); supervision (lead); writing – review and editing (supporting). **C. Thomas:** Data curation (lead); methodology (lead); writing – review and editing (supporting). **Ryan Vandermeulen:** Data curation (equal); writing – review and editing (supporting).

- Anning, T., MacIntyre, H. L., Pratt, S. M., Sammes, P. J., Gibb, S. & Geider, R. J. 2000. Photoacclimation in the marine diatom *Skeletonema costatum*. *Limnol. Oceanogr.* 45:1807–17.
- Arrigo, K. R., Mills, M. M., Kropuenske, L. R., van Dijken, G. L., Alderkamp, A. C. & Robinson, D. H. 2010. Photophysiology in two major Southern Ocean phytoplankton taxa: photosynthesis and growth of *Phaeocystis antarctica* and *Fragilariopsis cylindrus* under different irradiance levels. *Integr. Comp. Biol.* 50:950–66.
- Barton, S., Jenkins, J., Buckling, A., Schaum, C. E., Smirnov, N., Raven, J. A. & Yvon-Durocher, G. 2020. Evolutionary temperature compensation of carbon fixation in marine phytoplankton. *Ecol. Lett.* 23:722–33.
- Bracher, A., Vountas, M., Dinter, T., Burrows, J., Röttgers, R. & Peeken, I. 2009. Quantitative observation of cyanobacteria and diatoms from space using PhytoDOAS on SCIAMACHY data. *Biogeosciences* 6:751–64.
- Carreto, J. I., Seguel, M., Montoya, N. G., Clément, A. & Carignan, M. O. 2001. Pigment profile of the ichthyotoxic dinoflagellate *Gymnodinium* sp. from a massive bloom in southern Chile. *J. Plankton Res.* 23:1171–75.
- Casey, J. R., Aucan, J. P., Goldberg, S. R. & Lomas, M. W. 2013. Changes in partitioning of carbon amongst photosynthetic pico- and nano-plankton groups in the Sargasso Sea in response to changes in the North Atlantic Oscillation. *Deep Sea Res. 2 Top. Stud. Oceanogr.* 93:58–70.
- Chase, A. P., Boss, E., Cetinić, I. & Slade, W. 2017. Estimation of phytoplankton accessory pigments from hyperspectral reflectance spectra: toward a global algorithm. *J. Geophys. Res. Oceans* 122:9725–43.
- Chisholm, S. W., Frankel, S. L., Goericke, R., Olson, R. J., Palenik, B., Waterbury, J. B., West-Johnsrud, L. & Zettler, E. R. 1992. *Prochlorococcus marinus* nov. gen. nov. sp.: an oxyphototrophic marine prokaryote containing divinyl chlorophyll *a* and *b*. *Arch. Microbiol.* 157:297–300.
- Ciotti, A. M. & Bricaud, A. 2006. Retrievals of a size parameter for phytoplankton and spectral light absorption by colored detrital matter from water-leaving radiances at SeaWiFS channels in a continental shelf region off Brazil. *Limnol. Oceanogr. Methods* 4:237–53.
- Clementson, L. A. & Wojtasiewicz, B. 2019. Dataset on the absorption characteristics of extracted phytoplankton pigments. *Data Brief* 24:103875.
- Collins, M., Knutti, R., Arblaster, J., Dufresne, J., Fichet, T., Friedlingstein, P., Gao, X. et al. 2013. Long-term climate change: projections, commitments and irreversibility. In Stocker, T., Qin, D., Plattner, G., Tignor, M., Allen, S., Boschung, J., Nauels, A., Xia, Y., Bex, V. & Midgley, P. [Eds.] *Climate Change 2013: The Physical Science Basis. Contribution of Working Group I to the Fifth Assessment Report of the Intergovernmental Panel on Climate Change*. Cambridge University Press, Cambridge, UK, pp. 1029–136.
- Davison, I. R. 1991. Environmental effects on algal photosynthesis: temperature. *J. Phycol.* 27:2–8.
- Del Castillo, C. E., Signorini, S. R., Karaköylü, E. M. & Rivero-Calle, S. 2019. Is the Southern Ocean getting greener? *Geophys. Res. Lett.* 46:6034–40.
- Demmig-Adams, B. & Adams, W. W. I. 1992. Photoprotection and other responses of plants to high light stress. *Annu. Rev. Plant. Physiol. Plant. Mol. Biol.* 43:599–626.
- Dimier, C., Giovanni, S., Ferdinando, T. & Brunet, C. 2009. Comparative ecophysiology of the xanthophyll cycle in six marine phytoplanktonic species. *Protist* 160:397–411.
- DiTullio, G. R., Geesey, M. E., Maucher, J. M., Alm, M. B., Riesenman, S. F. & Bruland, K. W. 2005. Influence of iron on algal community composition and physiological status in the Peru upwelling system. *Limnol. Oceanogr.* 50:1887–907.
- Durbin, E. G. 1977. Studies on the autecology of the marine diatom *Thalassiosira nordenskiöldii*. II. The influence of cell size on growth rate, and carbon, nitrogen, chlorophyll *a* and silica content. *J. Phycol.* 13:150–5.
- Duyens, L. 1956. The flattening of the absorption spectrum of suspensions, as compared to that of solutions. *Biochim. Biophys. Acta* 19:1–12.
- Egeland, E., Guillard, R. & Liaaen-Jensen, S. 1997. Algal carotenoids. 63. Carotenoids from Prasinophyceae. 7. Additional carotenoid prototype representatives and a general chemosystematic evaluation of carotenoids in Prasinophyceae (Chlorophyta). *Phytochemistry* 44:1087–97.
- Egeland, E., Garrido, J., Clementson, L., Andresen, K., Thomas, C., Zapata, M., Ains, R., Llewellyn, C., Newman, G. & Rodríguez, F. 2011. Data sheets aiding identification of phytoplankton carotenoids and chlorophylls. In Roy, S., Llewellyn, C., Egeland, E. S. & Johnsen, G. [Eds.] *Phytoplankton Pigments: Characterization, Chemotaxonomy and Applications in Oceanography*. Cambridge University Press, Cambridge, UK, pp. 665–822.
- Eker-Develi, E., Kideys, A. E. & Tugrul, S. 2006. Effect of nutrients on culture dynamics of marine phytoplankton. *Aquat. Sci.* 68:28–39.
- Falkowski, P. G. 1994. The role of phytoplankton photosynthesis in global biogeochemical cycles. *Photosynth. Res.* 39:235–58.
- Falkowski, P. G. & LaRoche, J. 1991. Acclimation to spectral irradiance in algae. *J. Phycol.* 27:8–14.
- Falkowski, P. & Raven, J. A. 2007. *Aquatic Photosynthesis*. Princeton University Press, Princeton, NJ, 488 pp.
- Fawley, M. W. 1991. Disjunct distribution of the xanthophyll loroxanthin in the green algae (Chlorophyta). *J. Phycol.* 27:544–8.
- Feng, Y., Hare, C. E., Leblanc, K., Rose, J. M., Zhang, Y., DiTullio, G. R., Lee, P. A., Wilhelm, S. W., Rowe, J. M. & Sun, J. 2009. Effects of increased pCO₂ and temperature on the North Atlantic spring bloom. I. The phytoplankton community and biogeochemical response. *Mar. Ecol. Prog. Ser.* 388:13–25.
- Field, C. B., Behrenfeld, M. J., Randerson, J. T. & Falkowski, P. 1998. Primary production of the biosphere: integrating terrestrial and oceanic components. *Science* 281:237–40.

- Finenko, Z., Hoepffner, N., Williams, R. & Piontkovski, S. 2003. Phytoplankton carbon to chlorophyll *a* ratio: response to light, temperature and nutrient limitation. *Mar. Ecol. J.* 2:40–64.
- Fu, F. X., Warner, M. E., Zhang, Y., Feng, Y. & Hutchins, D. A. 2007. Effects of Increased temperature and CO₂ on photosynthesis, growth, and elemental ratios in marine *Synechococcus* and *Prochlorococcus* (Cyanobacteria). *J. Phycol.* 43:485–96.
- Gao, K. & Campbell, D. A. 2014. Photophysiological responses of marine diatoms to elevated CO₂ and decreased pH: a review. *Funct. Plant Biol.* 41:449–59.
- Garrido, J. L., Rodríguez, F. & Zapata, M. 2009. Occurrence of loroxanthin, loroxanthin decenoate, and loroxanthin dodecenoate in *Tetraselmis* species (Prasinophyceae, Chlorophyta). *J. Phycol.* 45:366–74.
- Geider, R., Osborne, B. & Raven, J. 1985. Light dependence of growth and photosynthesis in *Phaeodactylum tricornutum* (Bacillariophyceae). *J. Phycol.* 21:609–19.
- Graff, J. R., Milligan, A. J. & Behrenfeld, M. J. 2012. The measurement of phytoplankton biomass using flow-cytometric sorting and elemental analysis of carbon. *Limnol. Oceanogr. Methods* 10:910–20.
- Groß, E., Boersma, M. & Meunier, C. L. 2021. Environmental impacts on single-cell variation within a ubiquitous diatom: the role of growth rate. *PLoS One* 16:e0251213.
- Guillard, R. 1973. Division rates. In Stein, J. R. [Ed.] *Handbook of Phycollogical Methods: Culture Methods and Growth Measurements*. Cambridge University Press, London, pp. 289–311.
- Guillard, R. & Hargraves, P. 1993. *Stichochrysis immobilis* is a diatom, not a chrysophyte. *Phycologia* 32:234–6.
- Harrison, P., Conway, H., Holmes, R. & Davis, C. O. 1977. Marine diatoms grown in chemostats under silicate or ammonium limitation. III. Cellular chemical composition and morphology of *Chaetoceros debilis*, *Skeletonema costatum*, and *Thalassiosira gravida*. *Mar. Biol.* 43:19–31.
- Henriksen, P., Riemann, B., Kaas, H., Sørensen, H. M. & Sørensen, H. L. 2002. Effects of nutrient-limitation and irradiance on marine phytoplankton pigments. *J. Plankton Res.* 24:835–58.
- Hirata, T., Hardman-Mountford, N., Brewin, R., Aiken, J., Barlow, R., Suzuki, K., Isada, T., Howell, E., Hashioka, T. & Noguchi-Aita, M. 2011. Synoptic relationships between surface Chlorophyll-*a* and diagnostic pigments specific to phytoplankton functional types. *Biogeochemistry* 8:311–27.
- Holmes, D. T. & Buhr, K. A. 2007. Error propagation in calculated ratios. *Clin. Biochem.* 40:728–34.
- Hooker, S. B., Van Heukelem, L., Thomas, C. S., Claustre, H., Ras, J., Barlow, R., Sessions, H., Schlüter, L., Perl, J. & Trees, C. 2005. *The Second SeaWiFS HPLC Analysis Round-Robin Experiment (SeaHARRE-2)*. NASA Technical Memorandum 212785:124.
- Jeffrey, S. 1997. Qualitative and quantitative HPLC analysis of SCOR reference algal cultures. In Jeffrey, S., Mantoura, R. & Wright, S. [Eds.] *Phytoplankton Pigments in Oceanography*. UNESCO, London, pp. 343–60.
- Jeffrey, S., Wright, S. & Zapata, M. 2011. Microalgal classes and their signature pigments. In Roy, S., Llewellyn, C., Egeland, E. S. & Johnsen, G. [Eds.] *Phytoplankton Pigments: Characterization, Chemotaxonomy, and Applications in Oceanography*. Cambridge University Press, Cambridge, UK, pp. 3–77.
- Kiefer, D. A. & Cullen, J. J. 1991. Phytoplankton growth and light absorption as regulated by light, temperature, and nutrients. *Polar Res.* 10:163–72.
- Kulk, G., de Vries, P., van de Poll, W. H., Visser, R. J. & Buma, A. G. 2012. Temperature-dependent growth and photophysiology of prokaryotic and eukaryotic oceanic picophytoplankton. *Mar. Ecol. Prog. Ser.* 466:43–55.
- Lakeman, M. B., Von Dassow, P. & Cattolico, R. A. 2009. The strain concept in phytoplankton ecology. *Harmful Algae* 8:746–58.
- Latasa, M. 1995. Pigment composition of *Heterocapsa* sp. and *Thalassiosira weissflogii* growing in batch cultures under different irradiances. *Sci. Mar.* 59:25–37.
- Latasa, M., Scharek, R., Gall, F. L. & Guillou, L. 2004. Pigment suites and taxonomic groups in Prasinophyceae. *J. Phycol.* 40:1149–55.
- Laza-Martinez, A., Seoane, S., Zapata, M. & Orive, E. 2007. Phytoplankton pigment patterns in a temperate estuary: from unialgal cultures to natural assemblages. *J. Plankton Res.* 29:913–29.
- Leonardos, N. & Geider, R. J. 2004. Responses of elemental and biochemical composition of *Chaetoceros muelleri* to growth under varying light and nitrate: phosphate supply ratios and their influence on critical N: P. *Limnol. Oceanogr.* 49:2105–14.
- Letelier, R. M., Bidigare, R. R., Hebel, D. V., Ondrusek, M., Winn, C. & Karl, D. M. 1993. Temporal variability of phytoplankton community structure based on pigment analysis. *Limnol. Oceanogr.* 38:1420–37.
- Lewitus, A. J., White, D. L., Tymowski, R. G., Geesey, M. E., Hymel, S. N. & Noble, P. A. 2005. Adapting the CHEMTAX method for assessing phytoplankton taxonomic composition in southeastern US estuaries. *Estuaries* 28:160–72.
- Liefer, J. D., Garg, A., Fyfe, M. H., Irwin, A. J., Benner, I., Brown, C. M., Follows, M. J., Omta, A. W. & Finkel, Z. V. 2019. The macromolecular basis of phytoplankton C: N: P under nitrogen starvation. *Front. Microbiol.* 10:763.
- Litchman, E., de Tezanos Pinto, P., Edwards, K. F., Klausmeier, C. A., Kremer, C. T. & Thomas, M. K. 2015. Global biogeochemical impacts of phytoplankton: a trait-based perspective. *J. Ecol.* 103:1384–96.
- Liu, S., Yao, P., Yu, Z., Li, D., Deng, C. & Zhen, Y. 2014. HPLC pigment profiles of 31 harmful algal bloom species isolated from the coastal sea areas of China. *J. Ocean Univ. China* 13:941–50.
- Llewellyn, C. & Gibb, S. 2000. Intra-class variability in the carbon, pigment and biomineral content of prymnesiophytes and diatoms. *Mar. Ecol. Prog. Ser.* 193:33–44.
- Lohrenz, S. E., Weidemann, A. D. & Tuel, M. 2003. Phytoplankton spectral absorption as influenced by community size structure and pigment composition. *J. Plankton Res.* 25:35–61.
- Lomas, M., Bates, N., Johnson, R., Knap, A., Steinberg, D. & Carlson, C. 2013. Two decades and counting: 24-years of sustained open ocean biogeochemical measurements in the Sargasso Sea. *Deep Sea Res. 2 Top. Stud. Oceanogr.* 93:16–32.
- Low-Decarie, E., Fussmann, G. F. & Bell, G. 2011. The effect of elevated CO₂ on growth and competition in experimental phytoplankton communities. *Glob. Change Biol.* 17:2525–35.
- MacIntyre, H. L. & Cullen, J. J. 2005. Using cultures to investigate the physiological ecology of microalgae. In Andersen, R. A. [Ed.] *Algal Culturing Techniques*. Elsevier Academic Press, Cambridge, UK, pp. 287–326.
- Mackey, M., Mackey, D., Higgins, H. & Wright, S. 1996. CHEMTAX—a program for estimating class abundances from chemical markers: application to HPLC measurements of phytoplankton. *Mar. Ecol. Prog. Ser.* 144:265–83.
- Mackey, K. R., Paytan, A., Caldeira, K., Grossman, A. R., Moran, D., McIlvin, M. & Saito, M. A. 2013. Effect of temperature on photosynthesis and growth in marine *Synechococcus* spp. *Plant Physiol.* 163:815–29.
- Moore, L. R., Goericke, R. & Chisholm, S. W. 1995. Comparative physiology of *Synechococcus* and *Prochlorococcus*: influence of light and temperature on growth, pigments, fluorescence and absorptive properties. *Mar. Ecol. Prog. Ser.* 116:259–75.
- Moore, L. R., Coe, A., Zinser, E. R., Saito, M. A., Sullivan, M. B., Lindell, D., Frois-Moniz, K., Waterbury, J. & Chisholm, S. W. 2007. Culturing the marine cyanobacterium *Prochlorococcus*. *Limnol. Oceanogr. Methods* 5:353–62.
- O'Reilly, J. E. & Werdell, P. J. 2019. Chlorophyll algorithms for ocean color sensors-OC4, OC5 & OC6. *Remote Sens. Environ.* 229:32–47.
- O'Reilly, J. E., Maritorena, S., Mitchell, B. G., Siegel, D. A., Carder, K. L., Garver, S. A., Kahru, M. & McClain, C. 1998. Ocean color chlorophyll algorithms for SeaWiFS. *J. Geophys. Res. Oceans* 103:24937–53.

- Orr, J. C., Fabry, V. J., Aumont, O., Bopp, L., Doney, S. C., Feely, R. A., Gnanadesikan, A., Gruber, N., Ishida, A. & Joos, F. 2005. Anthropogenic ocean acidification over the twenty-first century and its impact on calcifying organisms. *Nature* 437:681–6.
- Richardson, T. L., Ciotti, Á. M., Cullen, J. J. & Villareal, T. A. 1996. Physiological and optical properties of *Rhizosolenia formosa* (Bacillariophyceae) in the context of open-ocean vertical migration. *J. Phycol.* 32:741–57.
- Rivero-Calle, S., Gnanadesikan, A., Del Castillo, C. E., Balch, W. M. & Guikema, S. D. 2015. Multidecadal increase in North Atlantic coccolithophores and the potential role of rising CO₂. *Science* 350:1533–7.
- Rodríguez, F., Chauton, M., Johnsen, G., Andresen, K., Olsen, L. & Zapata, M. 2006. Photoacclimation in phytoplankton: implications for biomass estimates, pigment functionality and chemotaxonomy. *Mar. Biol.* 148:963–71.
- Roy, S., Llewellyn, C. A., Egeland, E. S. & Johnsen, G. 2011. *Phytoplankton Pigments: Characterization, Chemotaxonomy and Applications in Oceanography*. Cambridge University Press, Cambridge, UK, 845 pp.
- Ruivo, M., Amorim, A. & Cartaxana, P. 2011. Effects of growth phase and irradiance on phytoplankton pigment ratios: implications for chemotaxonomy in coastal waters. *J. Plankton Res.* 33:1012–22.
- Sadeghi, A., Dinter, T., Vountas, M., Taylor, B., Altenburg-Soppa, M. & Bracher, A. 2012. Remote sensing of coccolithophore blooms in selected oceanic regions using the PhytoDOAS method applied to hyper-spectral satellite data. *Biogeosciences* 9:2127–43.
- Sakshaug, E., Johnsen, G., Andresen, K. & Vernet, M. 1991. Modeling of light-dependent algal photosynthesis and growth: experiments with the Barents sea diatoms *Thalassiosira nordenskiöldii* and *Chaetoceros furcellatus*. *Deep Sea Res. A* 38:415–30.
- Schaum, C. E., Rost, B. & Collins, S. 2016. Environmental stability affects phenotypic evolution in a globally distributed marine picoplankton. *ISME J.* 10:75–84.
- Schlüter, L., Möhlenberg, F., Havskum, H. & Larsen, S. 2000. The use of phytoplankton pigments for identifying and quantifying phytoplankton groups in coastal areas: testing the influence of light and nutrients on pigment/chlorophyll a ratios. *Mar. Ecol. Prog. Ser.* 192:49–63.
- Seoane, S., Laza, A. & Orive, E. 2006. Monitoring phytoplankton assemblages in estuarine waters: the application of pigment analysis and microscopy to size-fractionated samples. *Estuar. Coast. Shelf Sci.* 67:343–54.
- Signorini, S. R., Franz, B. A. & McClain, C. R. 2015. Chlorophyll variability in the oligotrophic gyres: mechanisms, seasonality and trends. *Front. Mar. Sci.* 2:1.
- Spilling, K., Ylöstalo, P., Simis, S. & Seppälä, J. 2015. Interaction effects of light, temperature and nutrient limitations (N, P and Si) on growth, stoichiometry and photosynthetic parameters of the cold-water diatom *Chaetoceros wighamii*. *PLoS One* 10:e0126308.
- Terry, K. L., Hirata, J. & Laws, E. A. 1985. Light-, nitrogen-, and phosphorus-limited growth of *Phaeodactylum tricornutum* Bohlin strain TFX-1: chemical composition, carbon partitioning, and the diel periodicity of physiological processes. *J. Exp. Mar. Biol. Ecol.* 86:85–100.
- Thompson, P. A., Guo, M. X. & Harrison, P. J. 1992. Effects of variation in temperature. I. On the biochemical composition of eight species of marine phytoplankton. *J. Phycol.* 28:481–8.
- Uitz, J., Claustre, H., Morel, A. & Hooker, S. B. 2006. Vertical distribution of phytoplankton communities in open ocean: an assessment based on surface chlorophyll. *J. Geophys. Res. Oceans* 111:C8.
- Van Heukelem, L. & Thomas, C. S. 2001. Computer-assisted high-performance liquid chromatography method development with applications to the isolation and analysis of phytoplankton pigments. *J. Chromatogr.* 910:31–49.
- Werdell, P. J., Behrenfeld, M. J., Bontempi, P. S., Boss, E., Cairns, B., Davis, G. T., Franz, B. A., Gliese, U. B., Gorman, E. T. & Hasekamp, O. 2019. The Plankton, Aerosol, Cloud, ocean Ecosystem mission: status, science, advances. *Bull. Am. Meteorol. Soc.* 100:1775–94.
- Wood, A. M. & Leatham, T. 1992. The species concept in phytoplankton ecology. *J. Phycol.* 28:723–9.
- Wood, A. M., Everroad, R. & Wingard, L. 2005. Measuring growth rates in microalgal cultures. In Andersen, R. A. [Ed.] *Algal Culturing Techniques*. Elsevier Academic Press, Cambridge, UK, pp. 269–86.
- Xu, K., Fu, F. X. & Hutchins, D. A. 2014. Comparative responses of two dominant Antarctic phytoplankton taxa to interactions between ocean acidification, warming, irradiance, and iron availability. *Limnol. Oceanogr.* 59:1919–31.
- Zapata, M., Rodríguez, F. & Garrido, J. L. 2000. Separation of chlorophylls and carotenoids from marine phytoplankton: a new HPLC method using a reversed phase C8 column and pyridine-containing mobile phases. *Mar. Ecol. Prog. Ser.* 195:29–45.
- Zapata, M., Edvardsen, B., Rodríguez, F., Maestro, M. A. & Garrido, J. L. 2001. Chlorophyll c2 monogalactosyldiacylglyceride ester (chl c2-MGDG). A novel marker pigment for Chrysochromulina species (Haptophyta). *Mar. Ecol. Prog. Ser.* 219:85–98.
- Zapata, M., Jeffrey, S., Wright, S. W., Rodríguez, F., Garrido, J. L. & Clementson, L. 2004. Photosynthetic pigments in 37 species (65 strains) of Haptophyta: implications for oceanography and chemotaxonomy. *Mar. Ecol. Prog. Ser.* 270:83–102.

Supporting Information

Additional Supporting Information may be found in the online version of this article at the publisher's web site:

Figure S1. Comparison of (A) But/Chl *a* and (B) But/C ($\mu\text{g} \cdot \text{mg}^{-1}$) values between *Karenia brevis*, *Pelagomonas calceolata* and But-containing haptophytes. Species names are on the *x*-axis, and ratio magnitude is on the *y*-axis. Circle diameter shows comparative biovolume between the taxa. Color indicates higher level taxonomic group.

Figure S2. Comparison of (A) Chl *b*/Chl *a* and (B) Chl *b*/C ($\mu\text{g} \cdot \text{mg}^{-1}$) values between *Bigelowiella natans* and the prasinophytes. Species names are on the *x*-axis, and ratio magnitude is on the *y*-axis. Circle diameter shows comparative biovolume between the taxa. Color indicates higher level taxonomic group.

Figure S3. Comparison of (A) Chl *c3*/Chl *a* and (B) Chl *c3*/C ($\mu\text{g} \cdot \text{mg}^{-1}$) values between diatoms, *Karenia brevis*, *Pelagomonas calceolata*, *Prasinococcus capsulatus* and the haptophytes. Species names are on the *x*-axis, and ratio magnitude is on the *y*-axis. Circle diameter shows comparative biovolume between the taxa. Color indicates higher level taxonomic group.

Figure S4. Comparison of (A) DVChl *b*/Chl *a* and (B) DVChl *b*/C ($\mu\text{g} \cdot \text{mg}^{-1}$) values between *Prochlorococcus marinus* and *Prasinococcus capsulatus*. Species names are on the *x*-axis, and ratio magnitude is on the *y*-axis. Circle diameter shows comparative biovolume between the taxa. Color indicates higher level taxonomic group.

Figure S5. Comparison of (A) Fuco/Chl *a* and (B) Fuco/C ($\mu\text{g} \cdot \text{mg}^{-1}$) values between the diatoms, *Karenia brevis*, the haptophytes and the raphidophytes. Species names are on the *x*-axis, and ratio magnitude is on the *y*-axis. Circle diameter shows comparative biovolume between the taxa. Color indicates higher level taxonomic group.

Figure S6. Comparison of (A) Hex/Chl *a* and (B) Hex/C ($\mu\text{g} \cdot \text{mg}^{-1}$) values between *Karenia brevis* and haptophytes. Species names are on the *x*-axis, and ratio magnitude is on the *y*-axis. Circle diameter shows comparative biovolume between the taxa. Color indicates higher level taxonomic group.

Figure S7. Comparison of (A) Zea/Chl *a* and (B) Zea/C ($\mu\text{g} \cdot \text{mg}^{-1}$) values between diatoms, *Bigelowiella natans*, the cyanophytes, the prasinophytes and raphidophytes. Species names are on the *x*-axis, and ratio magnitude is on the *y*-axis. Circle diameter shows comparative biovolume between the taxa. Color indicates higher level taxonomic group.

Table S1. Mean and standard deviation (SD) of Pig/Chl *a* ratios for the diatoms observed in this study, including pigment-based type, growth phase or treatment. Statistical significance is marked as: * $P < 0.05$, † = ranksum test. n.d. is not detected or below limit of quantitation.

Table S2. Mean and standard deviation (SD) of C/Chl *a* ($\mu\text{g} \cdot \mu\text{g}^{-1}$) and Pig/C ratios ($\mu\text{g} \cdot \text{mg}^{-1}$) for the diatoms observed in this study, including pigment-based type, growth phase or treatment. Statistical significance is marked as: * = difference is larger than the three-sigma limit. n.d. is not detected or below limit of quantitation.

Table S3. Mean and standard deviation (SD) of Pig/Chl *a* ratios for the *Bigelowiella natans* observed in this study during each growth phase. Statistical significance is marked as: * $P < 0.05$.

Table S4. Mean and standard deviation (SD) of C/Chl *a* ($\mu\text{g} \cdot \text{mg}^{-1}$) and Pig/C ratios ($\text{mg} \cdot \mu\text{g}^{-1}$) for *Bigelowiella natans* observed in this study during each growth phase.

Table S5. Mean and standard deviation (SD) of Pig/Chl *a* ratios for the cyanobacteria observed in this study, including pigment-based type, growth phase and treatment. Statistical significance is marked as: * $P < 0.05$, † = Wilcoxon rank sum test. n.d. is not detected or below limit of quantitation.

Table S6. Mean and standard deviation (SD) of C/Chl *a* ($\mu\text{g} \cdot \mu\text{g}^{-1}$) and Pig/C ratios ($\mu\text{g} \cdot \text{mg}^{-1}$) for the cyanobacteria observed in this study, including pigment-based type, growth phase or

treatment. Statistical significance is marked as * = difference is larger than the three-sigma limit. n.d. is not detected or below limit of quantitation.

Table S7. Mean and standard deviation (SD) of Pig/Chl *a* ratios for *Rhodomonas salina* observed in this study during each growth phase. Statistical significance is marked as: * $P < 0.05$, † = Wilcoxon rank sum test.

Table S8. Mean and standard deviation (SD) of C/Chl *a* ($\mu\text{g} \cdot \mu\text{g}^{-1}$) and Pig/C ratios ($\mu\text{g} \cdot \text{mg}^{-1}$) for *Rhodomonas salina* observed in this study during each growth phase.

Table S9. Mean and standard deviation (SD) of Pig/Chl *a* ratios for the dinoflagellates observed in this study, including pigment-based type and growth phase. Statistical significance is marked as: * $P < 0.05$, † = Wilcoxon rank sum test. n.d. is not detected or below limit of quantitation.

Table S10. Mean and standard deviation (SD) of C/Chl *a* ($\mu\text{g} \cdot \mu\text{g}^{-1}$) and Pig/C ratios ($\mu\text{g} \cdot \text{mg}^{-1}$) for the dinoflagellates observed in this study, including pigment-based type and growth phase. n.d. is not detected or below limit of quantitation.

Table S11. Mean and standard deviation (SD) of Pig/Chl *a* ratios for *Pelagomonas calceolata* observed in this study during each growth phase. Statistical significance is marked as: * $P < 0.05$, † = Wilcoxon rank sum test.

Table S12. Mean and standard deviation (SD) of C/Chl *a* ($\mu\text{g} \cdot \mu\text{g}^{-1}$) and Pig/C ratios ($\mu\text{g} \cdot \text{mg}^{-1}$) for *Pelagomonas calceolata* observed in this study during each growth phase. Statistical significance is marked as * = difference is larger than the three-sigma limit.

Table S13. Mean and standard deviation (SD) of Pig/Chl *a* ratios for the prasinophytes observed in this study, including pigment-based type, growth phase or treatment. Statistical significance is marked as: * $P < 0.05$, † = Wilcoxon rank sum test. n.d. is not detected or below limit of quantitation.

Table S14. Mean and standard deviation (SD) of C/Chl *a* ($\mu\text{g} \cdot \mu\text{g}^{-1}$) and Pig/C ratios ($\mu\text{g} \cdot \text{mg}^{-1}$) for the prasinophytes observed in this study, including pigment-based type, growth phase or treatment. Statistical significance is marked as * = difference is larger than the three-sigma limit. n.d. is not detected or below limit of quantitation.

Table S15. Mean and standard deviation (SD) of Pig/Chl *a* ratios for the haptophytes observed in this study, including pigment-based type,

growth phase or treatment. Statistical significance is marked as: * $P < 0.05$, † = Wilcoxon rank sum test. n.d. is not detected or below limit of quantitation.

Table S16. Mean and standard deviation (SD) of C/Chl *a* ($\mu\text{g} \cdot \mu\text{g}^{-1}$) and Pig/C ratios ($\mu\text{g} \cdot \text{mg}^{-1}$) for the haptophytes observed in this study, including pigment-based type, growth phase or treatment. Statistical significance between growth phases or treatment marked as * = difference is larger than the three-sigma limit. n.d. is not detected or below limit of quantitation.

Table S17. Mean and standard deviation (SD) of Pig/Chl *a* ratios for the raphidophytes observed in this study.

Table S18. Mean and standard deviation (SD) of C/Chl *a* ($\mu\text{g} \cdot \mu\text{g}^{-1}$) and Pig/C ratios ($\mu\text{g} \cdot \text{mg}^{-1}$) for the raphidophytes observed in this study. Statistical significance * = difference is larger than the three-sigma limit.

Table S19. Pigment $\cdot \text{cell}^{-1}$ in units of $\text{fg} \cdot \text{cell}^{-1}$ for all diatoms observed in this study including, pigment-based type, growth phase and treatment. n.d. = not detected or below the detection limit.

Table S20. Pigment $\cdot \text{cell}^{-1}$ in units of $\text{fg} \cdot \text{cell}^{-1}$ for *Bigeloviella natans* observed in this study during each growth phase.

Table S21. Pigment $\cdot \text{cell}^{-1}$ in units of $\text{fg} \cdot \text{cell}^{-1}$ for the cyanobacteria observed in this study including pigment-based type, growth phase and

treatment. n.d. = not detected or below the detection limit.

Table S22. Pigment $\cdot \text{cell}^{-1}$ in units of $\text{fg} \cdot \text{cell}^{-1}$ for *Rhodomonas salina* observed in this study during each growth phase.

Table S23. Pigment $\cdot \text{cell}^{-1}$ in units of $\text{fg} \cdot \text{cell}^{-1}$ for the dinoflagellates observed in this study including pigment-based type and growth phase. n.d. = not detected or below the detection limit.

Table S24. Pigment $\cdot \text{cell}^{-1}$ in units of $\text{fg} \cdot \text{cell}^{-1}$ for *Pelagomonas calceolata* observed in this study during each growth phase.

Table S25. Pigment $\cdot \text{cell}^{-1}$ in units of $\text{fg} \cdot \text{cell}^{-1}$ for the prasinophytes observed in this study including pigment-based type, growth phase and treatment. n.d. = not detected or below the detection limit.

Table S26. Pigment $\cdot \text{cell}^{-1}$ in units of $\text{fg} \cdot \text{cell}^{-1}$ for the haptophytes observed in this study including, pigment-based type and growth phase. n.d. = not detected or below the detection limit.

Table S27. Pigment $\cdot \text{cell}^{-1}$ in units of $\text{fg} \cdot \text{cell}^{-1}$ for the raphidophytes observed in this study.

Table S28. C $\cdot \text{cell}^{-1}$ and Carbon-per-biovolume ($\text{C} \cdot \mu\text{m}^{-3}$), strain number (No), pigment-based type, and growth phase or treatment for all phytoplankton strains observed in this study.